

390  
2-14-80

DR. 787

COO-2616-2(Pt.2)(Rev.2)

FURTHER INVESTIGATIONS OF DIFFUSER AUGMENTED WIND TURBINES  
PART 2 - TECHNICAL REPORT

Final Report

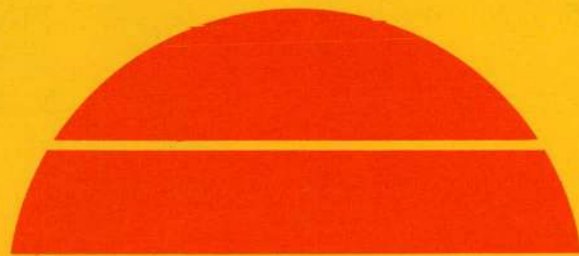
By  
K. M. Foreman  
B. L. Gilbert

July 1979

Work Performed Under Contract No. EY-76-C-02-2616

Research Department  
Grumman Aerospace Corporation  
Bethpage, New York

**MASTER**



**U.S. Department of Energy**

DISTRIBUTION OF THIS DOCUMENT IS UNLIMITED



**Solar Energy**

## DISCLAIMER

**This report was prepared as an account of work sponsored by an agency of the United States Government. Neither the United States Government nor any agency Thereof, nor any of their employees, makes any warranty, express or implied, or assumes any legal liability or responsibility for the accuracy, completeness, or usefulness of any information, apparatus, product, or process disclosed, or represents that its use would not infringe privately owned rights. Reference herein to any specific commercial product, process, or service by trade name, trademark, manufacturer, or otherwise does not necessarily constitute or imply its endorsement, recommendation, or favoring by the United States Government or any agency thereof. The views and opinions of authors expressed herein do not necessarily state or reflect those of the United States Government or any agency thereof.**

## **DISCLAIMER**

**Portions of this document may be illegible in electronic image products. Images are produced from the best available original document.**

## NOTICE

This report was prepared as an account of work sponsored by the United States Government. Neither the United States nor the United States Department of Energy, nor any of their employees, nor any of their contractors, subcontractors, or their employees, makes any warranty, express or implied, or assumes any legal liability or responsibility for the accuracy, completeness or usefulness of any information, apparatus, product or process disclosed, or represents that its use would not infringe privately owned rights.

This report has been reproduced directly from the best available copy.

Available from the National Technical Information Service, U. S. Department of Commerce, Springfield, Virginia 22161.

Price: Paper Copy \$5.25  
Microfiche \$3.00

DISCLAIMER

This book was prepared as an account of work sponsored by an agency of the United States Government. Neither the United States Government nor any agency thereof, nor any of their employees, makes any warranty, express or implied, or assumes any legal liability or responsibility for the accuracy, completeness, or usefulness of any information, apparatus, product, or process disclosed, or represents that its use would not infringe privately owned rights. Reference herein to any specific commercial product, process, or service by trade name, trademark, manufacturer, or otherwise, does not necessarily constitute or imply its endorsement, recommendation, or favoring by the United States Government or any agency thereof. The views and opinions of authors expressed herein do not necessarily state or reflect those of the United States Government or any agency thereof.

FURTHER INVESTIGATIONS OF DIFFUSER

AUGMENTED WIND TURBINES\*

PART II - TECHNICAL REPORT

by

K.M. Foreman and B.L. Gilbert

Research Department

Grumman Aerospace Corporation

Bethpage, New York 11714

July 1979

for

U.S. Department of Energy

Division of Solar Energy

Federal Wind Energy Program

\* This is a final report on DOE Contract No. EY-76-C-02-2616.M002 with the U.S. Department of Energy

Approved by:

*Richard A. Scheuing*  
Richard A. Scheuing  
Director of Research

THIS PAGE  
WAS THIS PAGE ALLY  
WAS INTENTIONALLY  
LEFT BLANK

TABLE OF CONTENTS

<u>Item</u>	<u>Page</u>
Introduction .....	2
Theory of Diffuser Augmentation .....	3
Diffuser Configurations .....	4
Experimental Program .....	5
Test Results .....	9
Economic Considerations .....	17
Concluding Remarks .....	19
Acknowledgments .....	20
References .....	20
 <u>Appendix</u>	
A     DAWT Engineering Design .....	23
B     DAWT Busbar Cost of Energy .....	47
C     Surface Pressure Distribution .....	51

LIST OF ILLUSTRATIONS

<u>Figure</u>		<u>Page</u>
1	Basic Schematic of the DAWT with Reference Stations .....	3
2	Schematic Representation of Flow Field for the Baseline DAWT Diffuser .....	5
3	DAWT Baseline Model Installation in the 2.1 x 3 m Wind Tunnel with Screen Simulation of a Turbine .....	6
4	DAWT Baseline Model Installation in the 2.1 x 3 m Wind Tunnel with Three-Bladed, Constant Chord Wind Turbine and Paraboloid Centerbody End Pieces .....	7
5	Diffuser Model Test Performance Trends with Screen Simulation of a Turbine ( $\lambda^{-1} = 2.78$ ) .....	11
6	Reynolds Number Effect on the Variation of Dynamic Pressure Ratio with Disk Loading for Two Diffuser Models ( $\lambda^{-1} = 2.78$ ) .....	12
7	Comparison of Baseline Diffuser Wind Tunnel Test Data with Turbines and Turbine Simulation by Screens .....	13
8	Comparison of Turbine Performance in the Wind Tunnel for Different Augmentation Systems .....	14
9	Centerline Augmentation Ratio Data of Several Ring Wing Diffuser Configurations at Different Disk Loadings .....	16
10	Centerline Data of Induced Dynamic Pressure Ratio at Turbine Face for Several Ring Wing Diffuser Configurations at Different Disk Loadings .....	16



## ABSTRACT

The Diffuser Augmented Wind Turbine (DAWT) is one of the advanced concepts being developed to improve the attractiveness of wind energy as an energy resource alternative. This work is dedicated to increase the concentration of naturally diffuse wind energy and reduce the specific cost of available power by minimizing the capital cost of energy conversion machinery.

Diffusers can increase turbine power output primarily by increasing mass flow rate through the blades because of controlled diffusion of the turbine wake which lowers the exit plane pressure considerably below atmospheric, and secondarily by reducing blade tip losses.

This paper describes a multiphased investigation, involving three test facilities, of several compact diffuser approaches. Screens, to simulate a wind turbine, and a three-bladed, fixed-pitch turbine have been used with the diffuser models. A candidate baseline design is described and some of the key issues are discussed that can lead to future full scale implementation.

## NOMENCLATURE

A	area
$c_b$	busbar cost of electricity
$C_C$	capital cost for rated power, Eq. (12)
$C_D$	diffuser cost
$C_F$	plant capacity factor
$C_{P_i}$	ideal power coefficient, Eq. (1)
$C_{P_R}$	diffuser pressure recovery coefficient
$C_{P_4}$	overall pressure recovery coefficient
$c_T$	turbine cost for low cost rotor construction
$c_{T_c}$	turbine cost for conventional rotor construction
$C_T$	rotor disk load, Eq. (5)
FCR	annual fixed charge rate
K	inlet total pressure loss
$L_i$	axial length of diffuser
OM	operations and maintenance costs
p	static pressure
$p_t$	total pressure
$P_{23}$	pressure drop across the turbine (rotor)
P	power
$q_0$	free stream dynamic pressure
$q_2$	local dynamic pressure at the rotor face
$r^2$	augmentation ratio, Eq. (3)
$\bar{r}$	weighted average augmentation ratio for rotor cross section
R	Reynolds Number (based on maximum diameter of diffuser)
$V^e$	wind velocity
$V_2^o$	axial velocity at the rotor face = $V_3$
$\alpha$	angle of attack of airfoil
$\beta$	turbine blade angle to plane of rotation
$\epsilon$	rotor station velocity ratio = $V_2/V_0$

$\eta_D$  diffuser efficiency  
 $\lambda$  diffuser throat-to-exit area ratio =  $A_2/A_4$   
 $\rho$  air density

Numbered subscripts refer to stations of reference diagram Fig. 1.

## INTRODUCTION

From simple momentum theory it can be shown that a maximum of only 59.3 percent of the natural wind energy contained in the swept area of a wind turbine's blades can be converted to shaft power. In reality, because of aerodynamic inefficiencies, the practical convertible fraction for conventional wind turbines is between 30 to 40 percent.

The Advanced and Innovative Concepts Project of the U.S. Department of Energy's Wind Energy Program is dedicated to improve the attractiveness of wind energy conversion systems (WECS) as an energy alternative by reducing the specific cost of available wind power by minimizing the capital cost of energy conversion machinery. The Diffuser Augmented Wind Turbine (DAWT) is one of these advanced concepts currently under development.

This application of diffusers has been considered and reconsidered periodically over the past 50 years (Ref. 1). Prior studies (Refs. 1, 2, 3) suffered from the economic burden of diffuser configurations that followed conventional wisdom. These designs were highly efficient, with small included angles (i.e., between 6 and 12 degrees) and very long. This early work has previously been summarized (Refs. 2, 4).

Our departure from tradition was to recognize that economic factors necessitate development of very short and compact diffusers. Thus, sacrifice of technical perfection is justified if the energy conversion system can produce low cost power.

The enclosure of a wind turbine by a diffuser produces increased power output by two independent processes:

- a) An increase in flow velocity (or mass) through the turbine blades by virtue of a controlled diffusion of the turbine wake, and
- b) A reduction in turbine blade tip losses.

Because of the potentially large gain possible from the first process, our primary concern is in this direction; tip loss reduction is an inherent secondary benefit.

This report describes our multiphased investigation of compact diffusers involving three test facilities and several design approaches. In our tests we have used screens to simulate a wind turbine, as well as a three-bladed, fixed-pitch turbine rotor assembly. Some of the critical issues that impact on performance-cost tradeoffs are discussed, and projections are presented to indicate the prospects for the DAWT concept.

## THEORY OF DIFFUSER AUGMENTATION

The one-dimensional momentum theory of DAWT augmentation was presented in Ref. 5. Referring to Fig. 1, the ideal power coefficient

$$C_{\mathcal{P}_i} = \Delta P_{23} V_2 / \frac{1}{2} (\rho V_o^3) \quad (1)$$

for the swept area of the turbine. The energy balance gives

$$C_{\mathcal{P}_i} = [1 - K_i - C_{P_4}] \epsilon - [1 - \eta_D (1 - \lambda)^2] \epsilon^3 \quad (2)$$

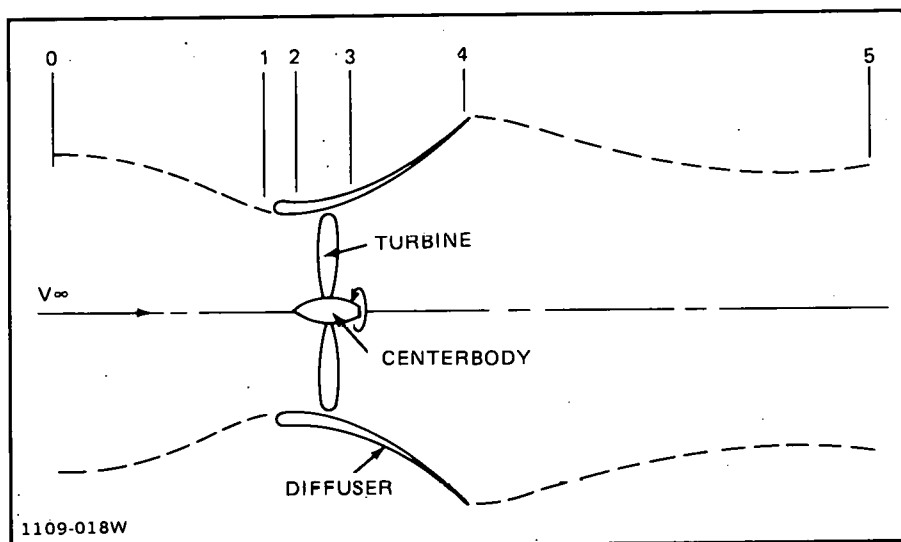


Fig. 1 Basic Schematic of the DAWT with Reference Stations

From Eq. (2) the power available to a perfect ducted turbine can be increased by small values for  $\lambda$ , high diffuser efficiency,  $\eta_D$ , a strongly negative base pressure coefficient,  $C_{P_4}$ , and an optimum rotor velocity ratio,  $\epsilon$ . The last parameter is dependent on rotor (or disk) loading ( $\Delta P_{23} / \frac{1}{2} \rho V_o^2$ ) of the turbine mounted in the diffuser.

The maximum (ideal) power coefficient of an unducted turbine is 16/27 (Ref. 1), the relative power coefficient,  $r$ , of the DAWT to the best unducted WECS is

$$r = \frac{27}{16} C_{\mathcal{P}_i} = \frac{C_{\mathcal{P}_i}}{0.593} \quad (3)$$

For equal turbine rotor sizes and free wind speeds,  $r$ , can be recast (Ref. 5) as:

$$r = \frac{C_T}{.593} \left( \frac{1 - C_{P_4}}{1 - C_{P_R} + C_T} \right)^{3/2} \quad (4)$$

where

$$C_T = \Delta P_{23} / \frac{1}{2} \rho V_2^2 \quad (5)$$

and

$$C_{P_R} = \frac{(P_4 - P_3)}{\frac{1}{2}(\rho V_3^2)} = \eta_D \left[ 1 - \left( \frac{A_3}{A_4} \right)^2 \right] \quad (6)$$

In Eq. (4), the inlet duct losses are combined with the overall diffuser pressure recovery coefficient,  $C_{P_R}$ . Experience (Ref. 3) indicates that the turbine load factor,  $C_T$ , is effectively uncoupled from  $C_{P_R}$ , so the maximum relative power coefficient, or augmentation ratio, is

$$r_{\max} = \frac{9}{8} (1 - C_{P_4}) \sqrt{\frac{1 - C_{P_4}}{3(1 - C_{P_R})}} \quad (7)$$

at an optimum rotor load of

$$(C_T)_{\text{OPT}} = 2 (1 - C_{P_4}) \quad (8)$$

The coefficients,  $C_{P_4}$ ,  $\epsilon$  and  $\eta_D$  must be determined empirically, so in practice the theory is semiempirical. Weighted averages of measured quantities at DAWT cross sections need to be obtained to properly evaluate DAWT performance.

The phenomenological explanation is that the greatly reduced (subatmospheric) pressure created behind the turbine by the diffuser causes more mass to flow through the DAWT, than an unducted rotor. Because wind power is the product of flow rate and turbine pressure drop, the resulting output of a given diameter turbine in a given wind velocity is increased significantly.

#### DIFFUSER CONFIGURATIONS

We have investigated two families of compact diffuser designs in our experimental program.

The first employs slot-injected external air to energize the boundary layer of the internal, or core flow. Figure 2 schematically indicates how the high energy air prevents core flow separation in the rapidly diverging boundary layer controlled (BLC) diffuser.

The second diffuser concept employs short ring airfoils. The low pressure distribution along the internal ring surface of high lift airfoil shapes induces augmented flow through the turbine if the latter is placed in a proper axial position. In addition to several different high lift contours and a staged series of rings, split flaps have been investigated for improved augmentation effect.

Other short axial length diffusers of segmented or nested arrangements have been reviewed. However, we believe these approaches are inherently quite costly to build in full scale versions. Accordingly, we have not investigated these other approaches beyond already published data.

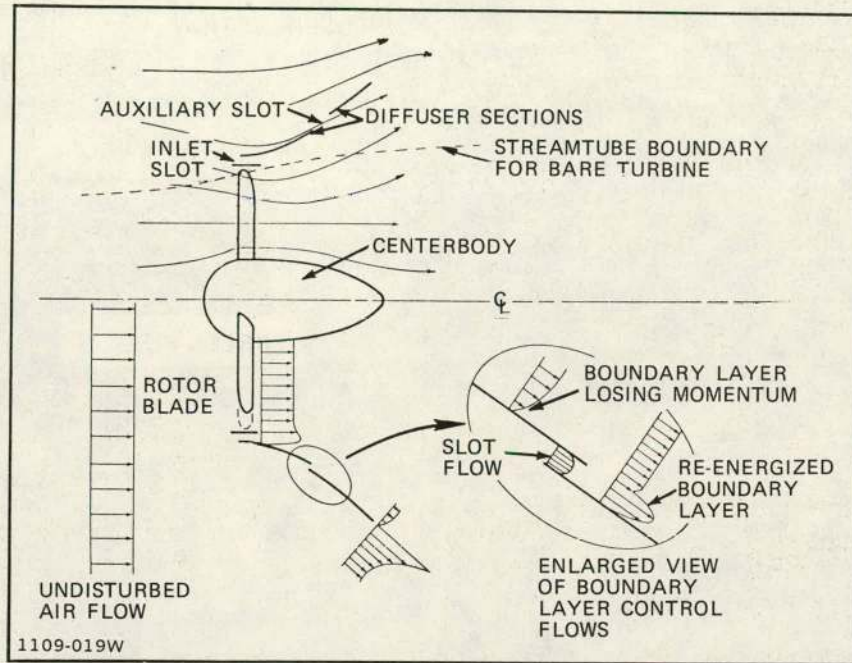


Fig. 2 Schematic Representation of Flow Field for the Baseline DAWT Diffuser

#### EXPERIMENTAL PROGRAM

Our investigation has been phased to provide an orderly cycle of performance data. The exploratory initial phase employed a 30 cm (11.5 in.) diameter open jet facility and 5 cm (2 in.) diameter inlet diffuser models. From over 150 different configurations of slotted BLC and ring wing models we selected a baseline design and three variants for further testing in a 2.1 x 3 m (7 x 10 ft) wind tunnel shown in Fig. 3. The geometrically similar models for this second phase have ten times larger diameter size and were subjected to three times higher wind speeds than previous tests.

In a third phase, the baseline diffuser installed in the 2.1 x 3 m (7 x 10 ft) wind tunnel was equipped with a fixed pitch, constant chord, three-bladed turbine instead of screens (see Fig. 4).

In the most recent or fourth phase models of the baseline and a previously tested variant diffuser were tested in a 1.2 x 1.8 (4 x 6 ft) meter wind tunnel. These intermediate size (15 cm (6 in.) inlet diameter) models employ screens and provide performance data for the basic configurations modified to improve low cost producibility prospects as well as at an intermediate test Reynolds Number. The logical future phase beyond facility-limited tests is implementation of a field test of a prototype size that would be meaningful for design performance evaluation in a real wind environment and for gaining fabrication methods and cost experience for an ultimate commercial product line.



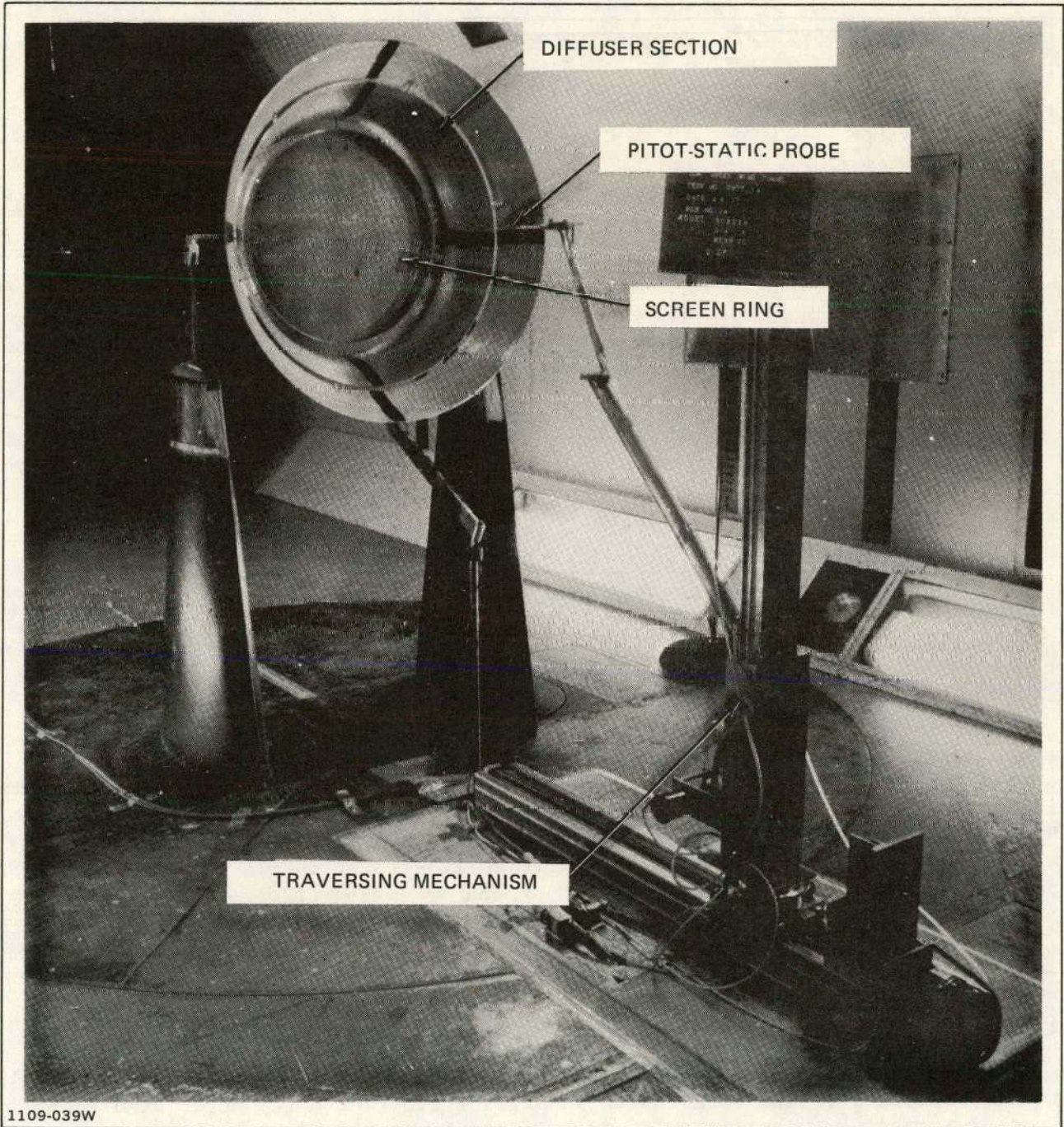


**Fig. 3 DAWT Baseline Model Installation in the 2.1 x 3 m Wind Tunnel with Screen Simulation of a Turbine**



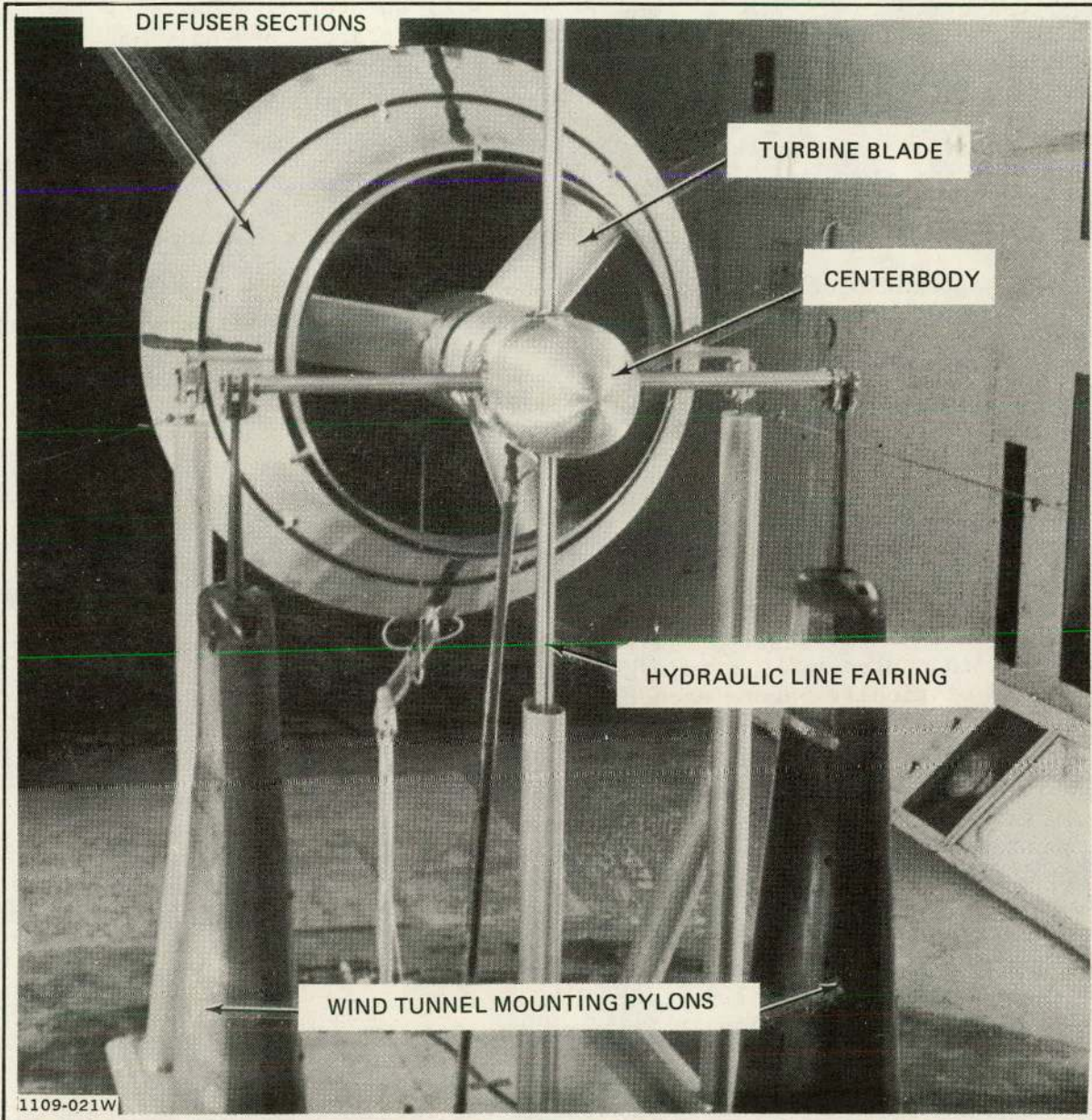


Fig. 4 DAWT Baseline Model Installation in the 2.1 x 3 m Wind Tunnel with Three-Bladed, Constant Chord Wind Turbine and Paraboloid Centerbody End Pieces. Turbine diameter is 18 in. (0.46 m).



## Turbine Simulation

It was impractical for us to fabricate a family of wind turbines for the exploratory, first phase investigation with 5 cm (2 in.) diameter inlet test models. Therefore, we simulated the turbine energy extraction with screens that dissipate through drag elements the air flow energy at the turbine position. Turbine performance can be represented by an overall local disk loading coefficient,  $C_T$ , defined by Eq. (5). The power extracted per unit area is the product indicated by the numerator of Eq. (1). The overall augmentation ratio,  $\bar{r}$ , for simulated turbine operation can be determined by

$$\bar{r} = \frac{C_T}{0.593} (q_2/q_0)^{3/2} \quad (9)$$

where  $q_2/q_0 = \left(\frac{V_2}{V_0}\right)^2$ , using test data about the screen disk loading and the measured average ratio of local-to-free stream velocity,  $V_2/V_0$ . The latter is obtained by pitot-static pressure probe surveys through the screens at several radial positions.

## Turbine Operation

Larger size models, used in the second and third phases, had a specially designed wind turbine positioned in the diffuser at the mean axial location of the screen (see Figs. 3 and 4). The total axial drag of the turbine is the summation of the blade and centerbody pressure drops at all turbine assembly surfaces. This force is measured by direct attachment to the wind tunnel's load cell measurement system through the mounting pylons. The torque produced by the turbine is measured by two flexure bars on the centerbody shell, each equipped with custom-built strain gages. This torque instrumentation is calibrated statically before each test series, and rechecked periodically.

The turbine blades are 15 cm long, 9.4 cm constant chord, NACA 63 (420)-422 airfoil contours (Ref. 8) machined from 7075-T6 aluminum. The blade section was selected because of its good lift to drag ratio ( $C_L/C_D \approx 120$  at  $C_L = 1.0$ ) and gentle stall properties which should minimize abrupt blade loading changes during off-design operation. Three blades are mounted 120 degrees apart in a machined aluminum hub of 15 cm (6 in.) diameter. A limited capability for  $\pm 3$  degrees change in blade angle from the mean position has been provided. This blade angle, however, cannot be changed during a dynamic test. Two shapes of centerbody end pieces have been tested, a paraboloid and a blunt profile. The turbine assembly was dynamically balanced to 3800 rpm, prior to formal testing, for all possible centerbody and blade angle combinations.

A hydraulic pump-motor is connected to the turbine shaft and enclosed within the centerbody shell fairing. This pump connects to a closed loop hydraulic system and provides the controllable load for the turbine. Turbine rpm can be varied by adjusting the hydraulic pressure drop across a control valve. Hydraulic lines pass from the centerbody to beneath the wind tunnel test section floor and to the control station and reservoir outside the wind tunnel's air flow passages.

A magnetic pickup in the turbine hub supplies the signal for rpm monitoring. The overall augmentation ratio for actual turbine operation is determined from



the axial force measurement and a measurement of turbine inlet velocity,  $V_2$ , by means of a static pressure manifold ring. Then

$$\bar{r} = \frac{\text{AXIAL FORCE}}{0.593 A_2 q_0} (V_2/V_0) \quad (10)$$

The turbine output shaft power is determined from the product of the measured torque and rpm.

## TEST RESULTS

In this section we present consolidated results of the three test phases for each of the two diffuser classes examined. To simplify presentation the test data have been reduced primarily to two evaluating parameters, 1) overall augmentation ratio,  $\bar{r}$ , defined by Eq. 3 and determined either by Eq. (9) where screens have been used to simulate a turbine, or by Eq. (10), where an actual turbine has been employed, and 2) the dynamic pressure ratio,  $q_2/q_0$ , which indicates the induced flow acceleration and the local flow conditions to be used for turbine design, compared to the natural wind conditions.

### Slotted Wall BLC Diffusers

The results of the initial small scale model, free jet flow facility investigation have been reported in detail in Refs. 6 and 7. Over 100 variations of wide angle slotted wall diffusers were constructed and tested. The power augmentation effect arises from increased mass flow through the turbine. This greatly enhanced core flow is due to the reduction of exit plane static pressure caused by accelerated external flow around the diffuser. The rise of internal flow static pressure is controlled by the diffuser to the subatmospheric exit plane value. An ideal conventional wind turbine would have a wake static pressure coefficient,  $C_{P4}$ , of  $-1/3$ . However, large included angle diffusers, of 60 to 80 degrees, have exit plane pressure coefficients of about  $-0.60$  to  $-0.90$  for operational Reynolds' numbers of  $10^4$  to  $10^6$ , respectively. The core flow then continues to expand freely and finally reach atmospheric pressure far downstream, (at greater than five exit diameters), while being re-energized by mixing with the surrounding natural wind.

The slotted diffuser's performance appears to be dependent on inlet geometry, the number and location of wall slots for introducing energetic external wind into the core flow boundary layer to suppress separation, size of the slots, turbine disk loading, diffuser angle, and Reynolds number of the overall flow process.

The conclusions of the initial (screen-equipped) test phase as presented in Ref. 7 are:

- A short constant area section is needed downstream of the turbine to initiate the core flow diffusion process against the adverse pressure gradient
- Power augmentation increases with diffuser area ratio to a maximum at a ratio of about 3

- General agreement with the observed performance data is obtained by a one-dimensional momentum theoretical model
- The presence of a ground plane seems to improve augmentation; with the exit plane within one-half a turbine diameter above the (simulated) ground, the augmentation increases by about 6 percent
- A combination of simulated wind profile and ground plane effects produces improved augmentation, up to 10 percent compared to a no boundary, uniform flow condition
- Centerbodies with cross-sectional areas up to about 10 percent of the turbine disk area produce very slight reduction in augmentation
- Small angular changes in pitch or yaw (to about 15 degrees) create minor variations in diffuser core flow.

Based on these test data and trends, a candidate baseline diffuser design was established for further investigation. In addition to its attractive performance, a peak augmentation ratio of about 1.9 at a local disk loading coefficient of 0.6, this three-element, compact design was judged qualitatively capable of easy manufacture and therefore cost effective. Features of the baseline design are: an included angle of 60 degrees, a length-to-inlet diameter ratio of about 0.5, and  $\lambda^{-1} = 2.78$  area ratio. The inlet slot sizing provides an initial boundary layer control airflow area that is 20 percent of the core flow area and a secondary slot located downstream provides additional tangential airflow, equal to 8 percent relative to the core flow, to re-energize further the boundary layer.

In a second phase, the baseline diffuser design was tested by a ten-times larger geometric scale model in a 2.1 x 3 m (7 x 10 ft) wind tunnel (Fig. 3). For a test Reynolds number up to 35 times greater than the initial (small scale) test series, the results indicate about a 10 percent further improvement in augmentation ratio at a  $C_T \approx 0.6$ ; these data show the weak but positive performance sensitivity to Reynolds number when screens are used to simulate turbines.

Three other diffuser designs also were tested in this second phase; they are essentially variants of the baseline configuration guided by the research of flow separation suppression by sequential wall jets (Ref. 9). In model 2 (a four component design) the rear section of the baseline configuration is changed into two separate sections, each with one half the running length of the baseline component; the height of the bleed air slot at the upstream entrance of each of the shorter sections is one-half that of the baseline model.

The five-element diffuser making up the model 3 design employs a shortened initial shroud (by 50 percent) and three auxiliary diffuser stages each preceded by a bleed air slot of one-third the height of the baseline design. Model 3 also is about 6 percent shorter in axial length than the baseline design for the same overall area ratio. The last diffuser design variant, model 4, has a main (initial) duct component one-third shorter than the baseline design and three auxiliary diffuser stages, each preceded by a slot of one-

half the height of the baseline design. Thus, the total bleed air used in model 4 adds 32.5 percent to the core flow and the main slot supplied almost two-thirds of this bleed air. (All four models have identical main (initial) slot geometries.)

Two of these screen-equipped diffuser models were investigated for two ( $\lambda^{-1}$ ) overall area ratios. At a common reference  $C_T$  of 0.6, model 2 exhibits 9.5 percent better augmentation than the baseline model, and model 4 about 2.5 percent poorer performance. For a 10 percent reduction in area ratio, model 4's augmentation ratio suffers a 13.5 percent loss and model 3 has 8.5 percent lower performance than model 4.

These results suggest that the major measure for suppression of core flow separation in our high angled diffuser designs is the initial, channelled annular flow around the turbine. Premature or large injection amounts of secondary bleed air become less effective than more frequent, but smaller quantities of wall flow. Finally, the three-wall jet arrangement (model 2) with sequential kinetic energy fluxes of approximately 70, 15, and 15 percent appears to be the best configuration of those tested; this result is generally consistent with North's findings (Ref. 9).

Figure 5 summarizes some of the screen-equipped diffuser results (except for model 3) described previously. In addition, the results of an intermediate size model test series are shown for a Reynolds number twice that of the first phase.

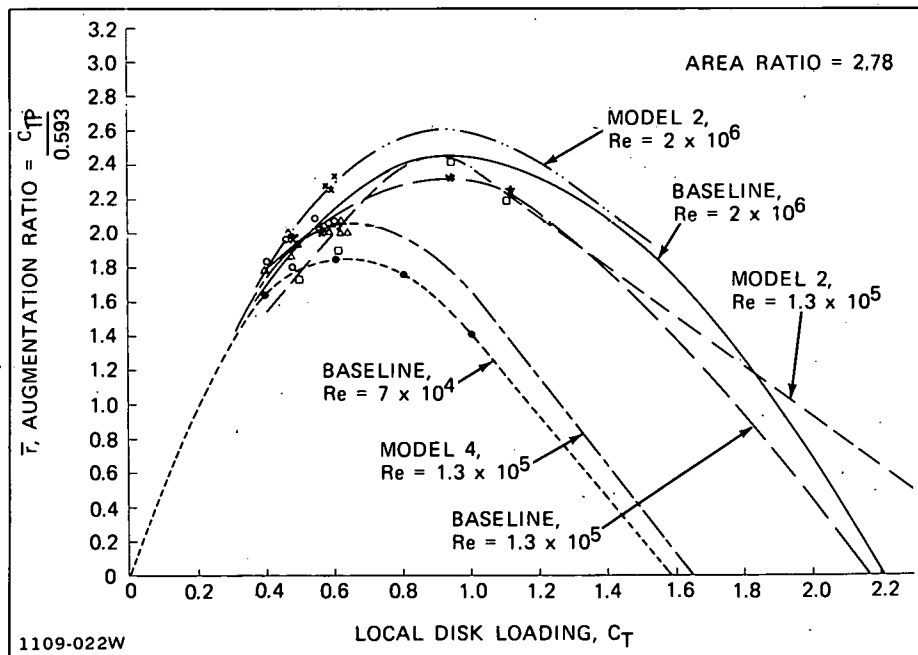


Fig. 5 Diffuser Model Test Performance Trends with Screen Simulation of a Turbine ( $\lambda^{-1} = 2.78$ )

The extrapolation of the curves of Fig. 5 beyond the  $C_T \approx 1.1$  data limit results from the use of Eq. (9) and the data of Fig. 6. Curve-fitting the variation of  $(q_2/q_0)$  test data with  $C_T$  (Fig. 6) yields quasi-linear relationships for baseline designs, with increasing  $(q_2/q_0)$  ratio as  $C_T$  decreases. The augmentation ratio then has an approximately parabolic variation with  $C_T$

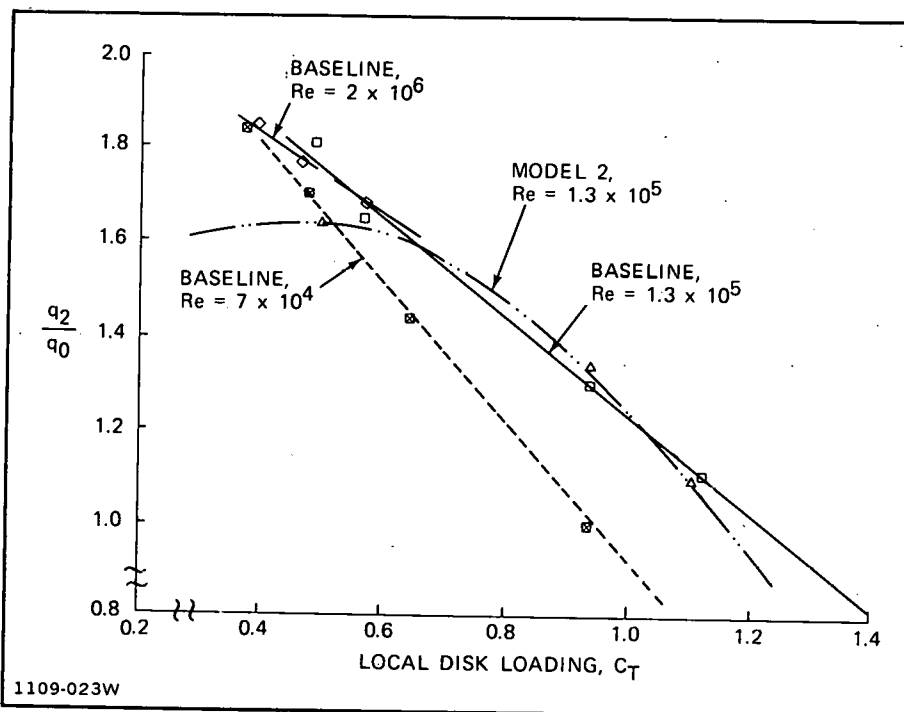


Fig. 6 Reynolds Number Effect on the Variation of Dynamic Pressure Ratio with Disk Loading for Two Diffuser Models ( $\lambda^{-1} = 2.78$ )

and an optimum  $\bar{r}$  and  $C_T$  can be computed, as is shown by Fig. 5; the zero value limits to  $\bar{r}$  indicated are academic because for all practical purposes interest in the diffuser will be lost below an augmentation of 1.0.

The point should be made that the DAWT performance in Fig. 5 is compared to an ideal actuator disk theory; real performance of an unducted turbine will be considerably lower than the ideal 0.593 power coefficient value. The DAWT, however, also has to employ a real turbine and the relative real performance is likely to be proportional to the relative ideal performance.

In contrast to a slowdown of 33 percent of the wind speed at the turbine's upstream face, for optimum unducted rotors, Fig. 6 shows that the diffuser produces considerable speedup of the local flow approaching the turbine. This condition allows the turbine to come on-stream at lower natural wind speeds than conventional rotors, and reach rated power output faster.

Another result of the testing with a turbine simulated by screens of several pressure loss factors has been the confirmation of a highly subatmospheric exit plane pressure that is essentially invariant with disk loading (Ref. 3). At the highest Reynold's number tested,  $C_{P_4}$  is about 42 percent lower (i.e., more subatmospheric) than at the lowest Re test conditions.

In a third test phase, the baseline diffuser was tested with a working turbine. Large improvements in measured DAWT performance were in evidence, as shown by Fig. 7. Two centerbody shapes and two constant blade angle values were examined.

Over the range tested, the disk loading varies nearly inversely linear with turbine speed ratio and with dynamic pressure ratio,  $q_2/q_0$ . Peak aug-

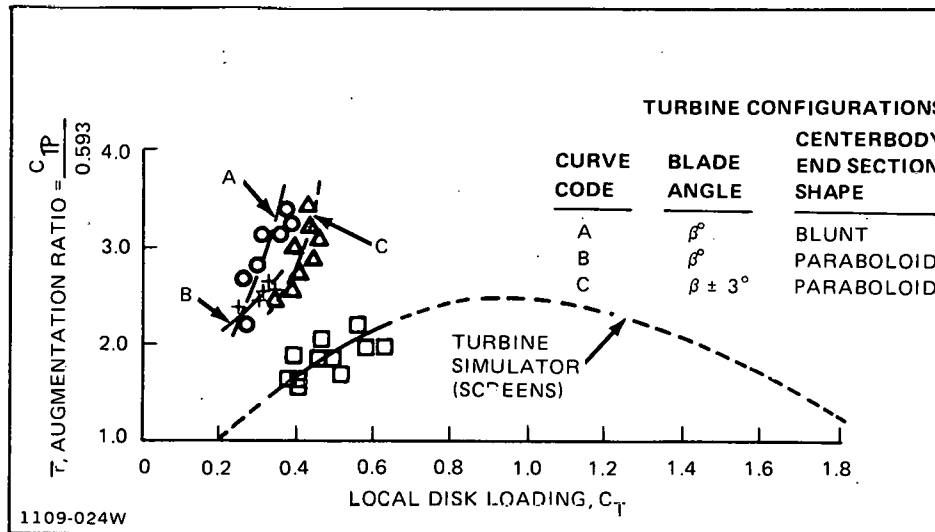


Fig. 7 Comparison of Baseline Diffuser Wind Tunnel Test Data with Turbines and Turbine Simulation by Screens

mentation ratio obtained for the near-unity speed ratio is 3.4 when referenced to the ideal, infinite speed ratio, power coefficient of 0.593; the accompanying local disk loading is about 0.42. Higher  $C_T$  values were precluded by testing limitations and turbine design assumptions based on the screen tests. Making the reasonable assumption that the activator disk theory of conventional base turbines is applicable to the DAWT application, the power coefficient of 2.02 obtained by the tested DAWT system would have been increased to at least 2.77 if the turbine had been able to operate at a speed ratio of 5 or 6, which is more characteristic of modern wind turbine practice; the ratio of ideal turbine efficiencies at speed ratios of 5. and 1. is (0.96/0.70) or 1.37. Then, for the more efficient turbine operation, the expected augmentation ratio is almost 4.7 at  $C_T \approx 0.4$ . Further, if the trend of  $\bar{r}$  variation with  $C_T$  is followed as given by the curves shown in Figs. 5 and 7 for screen data, a peak augmentation ratio of about 6.3 would be expected at an optimum disk loading of approximately 0.9.

The turbine wake (swirl) mixing with the diffuser's boundary layer apparently enhances the momentum exchange of slot flow at the walls and produces a more efficient diffuser than obtained using screens of the same disk loading coefficient.

The measured relative merit of the DAWT to the bare turbine at their respective test speed ratios is shown in Fig. 8. The peak power coefficient of the DAWT is over 3.8 times greater than that of the bare turbine. Enclosing the turbine within a simple short cylindrical duct (length/diameter ratio of 0.5) yields slightly better than twice the bare turbine power as shown in Fig. 8. The cylinder acts as a low (1.09) area ratio diffuser and inhibits turbine tip losses.

The conclusions evident from our turbine operational experience are:

- For the same disk loading (i.e.,  $C_T \approx 0.4$ ) the turbine-equipped DAWT gives two times the power coefficient of a screen-equipped diffuser of the baseline design

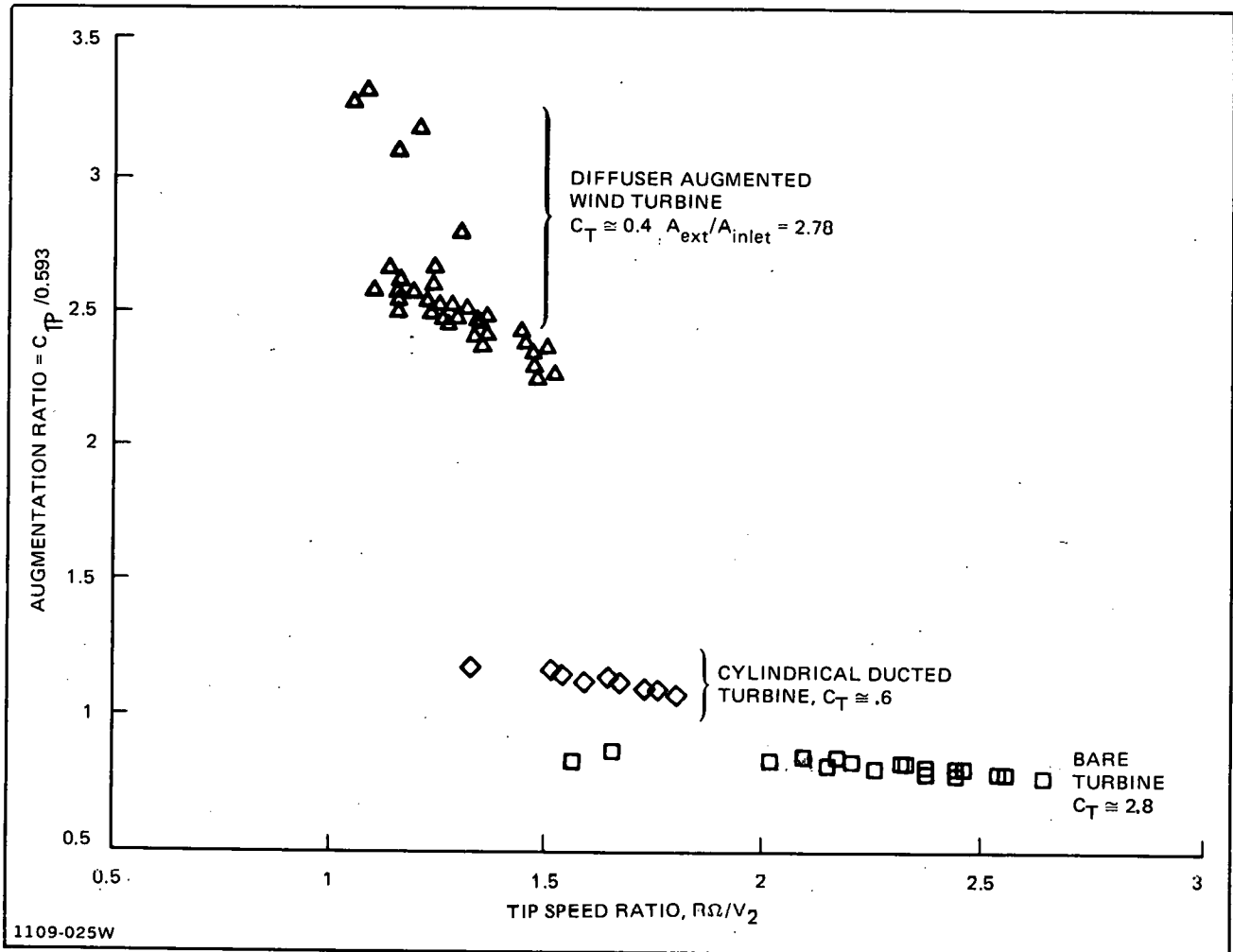


Fig. 8 Comparison of Turbine Performance in the Wind Tunnel for Different Augmentation Systems

- For the same turbine speed ratio, the baseline diffuser produces almost four times the power of a bare turbine and almost three times the power of a short cylindrical ducted turbine
- The swirl of the turbine wake produces a more efficient diffusion process in high-included angle, short diffusers, than is possible only with boundary layer separation suppression measures of screen-equipped diffusers.

The three-boundary layer slot diffuser configuration, represented by model 2, offers 10 percent performance improvement over the two slotted baseline design which could bring possible peak augmentation ratio values above 7.0 for a DAWT with turbine speed ratio above 5. The complication of assembling an additional diffuser segment in the field is judged, on a preliminary qualitative basis, as not a cost-effective move. In this fluids engineering application, minor technical improvements are not justified if accompanied by cost increments. However, a detailed point engineering design and cost estimate is required before final judgement is made.

The ring wing diffuser concept is based on the chordwise pressure distribution along the surfaces of airfoil contours; low pressures exist along the upper surface and high pressures along the lower surface. In a ring wing diffuser, the inner surface corresponds to the normally low pressure contour.

Three airfoil contours have been investigated using small scale metal models: 1) a moderately thick cambered NACA 4412 section (Ref. 8); 2) the high lift Williams airfoil "A" (Ref. 10); and 3) the high lift Liebeck laminar rooftop design (Ref. 11). The effect of energy dissipation by screen drag (to simulate turbine energy extraction) on the gross ring wing flow field has been measured empirically. Screens of various solidities were mounted at several different axial positions relative to the diffuser throat (minimum cross section) to examine optimum location. Furthermore, various split flap and staged airfoil flap arrangements were investigated for the effect of their lift enhancement (Ref. 6) on power augmentation ratio.

For the NACA 4412 and Williams "A" contour diffusers, it has been observed that a screen position at about the 75 percent chord position yields greater power augmentation results than if located near the leading edge, minimum cross section, or within five percent chord of the trailing edge.

The variation of augmentation ratio with disk loading for four ring wing diffuser configurations is summarized by Fig. 9. Also spotted are data points for five other configurations. The diffusers with 90 degree split flaps have 20 to 45 percent higher performance than the basic ring wing. The ring wing equipped with an airfoil flap exhibits 88 percent performance improvement over the basic ring wing and 50 percent better than the split-flap equipped diffuser. Normally, the higher lift coefficient attained at higher angles of attack,  $\alpha$ , (below stall condition) would mean that a ring wing at  $\alpha = 12$  degrees would have superior performance than one at  $\alpha = 6$  degrees, for comparable geometries. Indeed, the two data points comparing ring wing configurations 1a and 2a, in Fig. 9, do follow expected trends. However, the split flap shifts the stall angle of the airfoil to a lower angle of attack than the basic contour. Therefore, the diffuser with a flapped NACA 4412 ring wing at  $\alpha$  of 12 degrees exhibits lower performance than at an  $\alpha = 6$  degrees attitude, because the stall angle is shifted to slightly below 12 degrees by the flap.

The Williams "A" contour diffuser produces similar but slightly lower performance than the NACA 4412 ring wing diffuser, for flapped versions. The unflapped ring wing yields better results for the Williams "A" contour presumably because its peak lift coefficient is greater than for the NACA 4412. The short axial length of the Williams contour, however, for equal diffuser expansion ratios gives it an advantage over the standard NACA 4412 airfoil lines.

The induced dynamic pressure ratio trends for the tested ring wings is displayed in Fig. 10 over a range of disk loadings. The general trend is for turbine approach velocities to be greater than the free wind for low to moderate turbine disk loadings. At  $C_T$  values above 0.7 to 0.8, the local dynamic pressure is less than the free wind, at the turbine's upstream face. Clearly, the ring wing diffusers induce higher mass flows through the turbine plane than for an optimum unshrouded turbine, or a simple cylindrical ducted turbine (see test data point on Fig. 10).

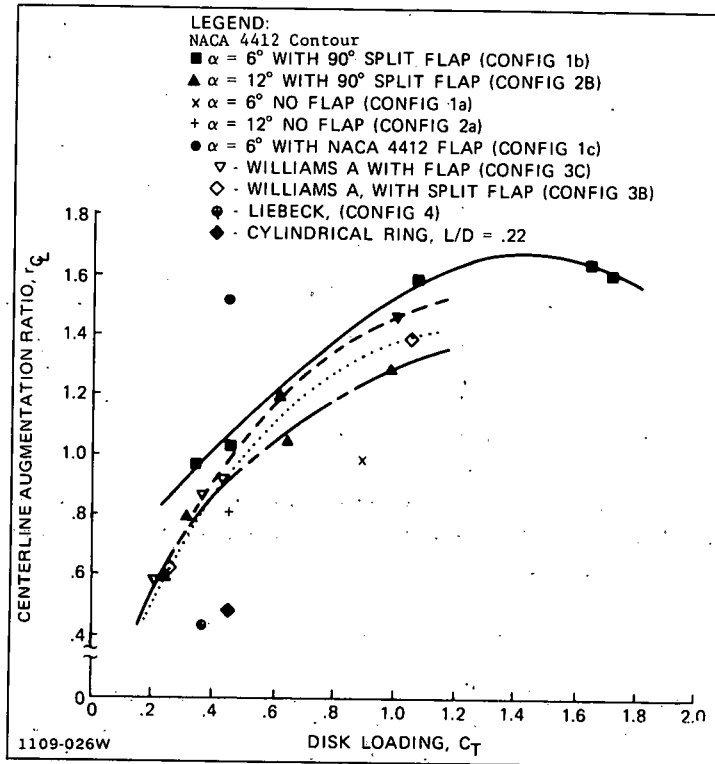


Fig. 9 Centerline Augmentation Ratio-Data of Several Ring Wing Diffuser Configurations at Different Disk Loadings. Data taken at nominal Reynolds Number of  $7 \times 10^4$ .

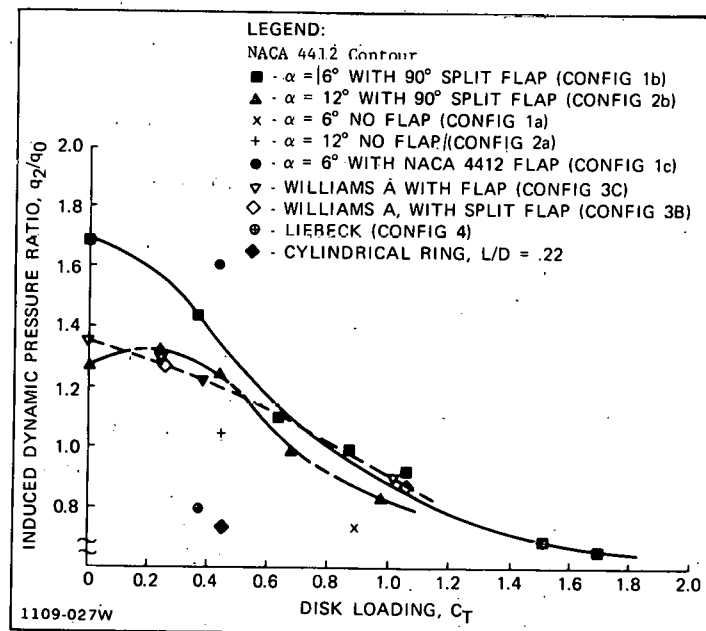


Fig. 10 Centerline Data of Induced Dynamic Pressure Ratio at Turbine Face for Several Ring Wing Diffuser Configurations at Different Disk Loadings. Data taken at nominal Reynolds Number of  $7 \times 10^4$ .



The disappointing test results obtained with the Liebeck contour ring diffuser at one low disk loading condition (see Figs. 9 and 10) led us to abandon further investigation. A simple short cylindrical tube offers as much benefits as the more structurally massive Liebeck contour, despite the latter's very high lift potential.

The exit plane pressure data for the short ring wing diffusers indicate highly subatmospheric pressures, with  $C_p$  between -0.60 and -0.70. These are comparable with the best of the long diffuser designs reported by Igra (Ref. 3), and could not have been predicted a priori.

On the basis of this small scale model investigation, the technical performance of the short flapped ring wing diffuser appears attractive for power augmentation of highly loaded wind turbines. Performance projections to larger model sizes, operating Reynolds Number, and to turbine use instead of screens, give this class of diffusers values of augmentation ratios comparable to the best of the multislot (BLC) types. However, from a preliminary consideration of the fabrication cost and material bulk requirements to assure construction fidelity to the airfoil contours, we judge ring wing diffusers to be less cost effective than the slotted wall, high-included angle conical diffusers represented by the baseline design. This evaluation could change if nonmetallic construction were considered (e.g., reinforced concrete) and if appreciable cross section thickness were necessary to maintain structural integrity.

#### ECONOMIC CONSIDERATIONS

Early economic studies (Refs. 4 and 6) of DAWT applications identified two areas of cost effectiveness. The first was for very large multimegawatt units where rotor system cost is a major part of the overall WECS investment. When only be achieved by inordinately large increases in rotor cost (because of aeroelastic stress escalation), the diffuser can become a cheaper alternative. However, this assumes that the manufacture, transportation to and erection at the field installation site of the diffuser results in lower overall cost for the DAWT's generated power.

The second application area is where the DAWT can extend the power rating range of low cost rotor construction technology. A size limitation occurs because of aeroelastic loading limits. Then, the diffuser provides an alternative to the use of more expensive rotor construction approaches for larger diameter, higher power rating, units or the replicating of the low cost technology units. Because the wind energy field lacks broad modern experience and current hard cost data, all paper studies of costs suffer lack of credibility. However, some guidance relative to the controlling economics can be obtained by the following discussion.

#### Busbar Costs

Assuming that a DAWT can be rated at  $\bar{r} P$  (power output) by virtue of its augmentation ratio, then the incremental cost of the diffuser offers the equivalent power rating of  $(\bar{r} - 1)$  additional, unducted, conventional turbines of the same diameter used by the DAWT. An additional feature of DAWT operation is the improvement in plant capacity factor because of the wind speedup at the turbine over the free wind velocity; in contrast, the local flow velocity at

a bare turbine is less than the free wind speed. For operational parameters of small commercial wind turbines, in an average wind variance environment, the DAWT typically has 150 percent the annual capacity factor of conventional machines. Therefore, the annual energy output of the DAWT will be  $(1.5\bar{r}-1)$  greater than conventional WECS of the same rotor diameter and free wind speed.

The busbar cost of electrical power is the ultimate basis for cost competitiveness of wind energy converters. For nonstorage type applications, the busbar cost,  $c_b$ , can be estimated (Ref. 12) by

$$c_b = \frac{C_C \times \text{FCR}}{C_F \times 8.76} + \text{OM}, \quad \text{mills/kWh} \quad (11)$$

where FCR and OM are not dependent on the wind energy conversion system. An approximate indication of where the breakeven point is reached for the DAWT compared to the conventional WECS is when the ratio  $C_C/C_F$  is the same for both approaches. Excluding foundation and electrical hookup costs, the capital cost of the DAWT is

$$C_C = \frac{c_D + c_T}{\bar{r} P} \quad (12)$$

but the DAWT can have 150 percent greater  $C_F$  than conventional WECS at low average wind speed sites. Then,

$$\frac{\text{DAWT } c_b}{\text{WECS } c_b} = \frac{c_D + c_T}{c_T} \times \frac{P}{\bar{r} P} \times \frac{1}{1.5} = \frac{1}{1.5\bar{r}} \left( \frac{c_D}{c_T} + 1 \right) \quad (13)$$

For a nominal augmentation ratio of 4, the DAWT will provide cheaper power if

$$c_D \lesssim 5 c_T$$

This criterion sets a cost target for the diffuser, if the same turbine technology costing rules apply in the comparison.

If the DAWT, using low cost rotor technology, is compared under the same assumptions as previously to a larger turbine of equal power rating but of higher cost construction, then the DAWT provides cheaper busbar power costs approximately when:

$$c_D \lesssim 1.5 c_{T_c} - c_T$$

For  $\bar{r} = 4$  and if  $c_{T_c} \approx 2 c_T$ , the diffuser capital cost can be

$$c_D \lesssim 2 c_T$$

or

$$c_D \lesssim c_{T_c}$$

to be cost competitive with conventional WECS. To give this analysis a sense of reality, the 38 m (125 ft) diameter rotor for the 200 kW rated, Mod-OA

prototype WECS installed in 1978 at Clayton, New Mexico, cost over \$500,000 (the entire WECS was estimated to cost over \$1.2 million (Ref. 13)). In this case a DAWT of comparable rated power would have a cost target of \$500,000 or less for the diffuser, and an additional allowance of \$250,000 for a 19 m (62.5 ft) diameter, cheaper technology, turbine in order to yield equal busbar costs of power.

### Principal Issues

The key issues affecting commercialization of the DAWT are: a) annual energy delivered, b) siting, c) design approach, and d) manufacturing approach.

These issues are interacting and have a profound influence on the final cost of a marketable diffuser.

The size is interrelated with the rotor design and the market need for wind energy systems. The siting issue is concerned with the wind characteristics such as annual speed distribution and direction, accessibility for installation and maintenance, the proximity to and nature of the market for the DAWT's output, and the weather environment. These conditions also affect the diffuser design in establishing environmental and operational factors. Other design issues are the criteria to be used for structural loading and deflection; for the latter, particularly, the needed clearance around the rotating turbine. Materials selection also will have a large influence on the design as well as the manufacturing issue.

The essence of the manufacturing issue is economics, not technology. Some of the variables that must be considered are: fabrication method, diffuser size, locality and accessibility of market sites, and proximity of the fabrication site to the market. Also important are the quality and availability of the labor supply and construction materials, and the shipping restrictions relating to unit size and weight that must be considered in planning fabrication and design approaches.

### CONCLUDING REMARKS

This concise summary has traced the considerable progress made during the past three years in developing short, cost-effective diffusers for wind energy conversion applications. The major effort has been experimental with theoretical guidance provided by a one-dimensional fluid dynamics model. An outcome of this work has been the definition of a baseline diffuser configuration. Combined with a working but not optimized turbine, wind tunnel tests have demonstrated the ability of this configuration to produce almost 3.5 times the ideal power coefficient of a conventional wind turbine of the same size. The employment actuator disk and diffuser theoretical models, projections from these data to better turbine operating speed ratios and disk loading, and to improved diffuser configurations, promises power coefficients over six times the best of conventional wind turbines, and about ten times more annual energy delivered.

Incidental to this investigation has been the determination that screens are inexpensive simulators of wind turbines but that they severely underestimate the performance of the rotor-diffuser system because of the absence of turbine swirl wake effects.

The power generation market puts a high value on inexpensive capital equipment in preference to small technical refinements in fluids engineering. It is recognized that the lack of an operational experience base for estimating DAWT diffuser cost makes any paper studies suspect. Such rough estimate studies have provided a basis for expecting DAWT busbar costs to be comparable to current fossil fuel generation performance. Unfortunately these predesign paper studies and their economic conclusions are a needed prerequisite to qualify for the attention leading to implementation outside the laboratory. Meaningful field tests are needed where the natural long term wind environment and the physical visibility and documented performance of real power producing equipment will provide credibility to the developer's claims.

#### ACKNOWLEDGMENTS

This work was supported by the Wind Systems Branch, Solar Technology Division, of the U.S. Department of Energy under contract no. EY-76-C-2-2616. The authors express their appreciation to Dr. R.A. Oman for his contribution in the conceptual and early experimental phases of this project and his continued interest and guidance in the later phases. We also thank Dr. Peter Moretti, DoE contract technical monitor, for his consultation and guidance.

#### REFERENCES

1. Betz, A., "Energienutzungen in Venturidusen," Naturwissenschaften, Vol. 10, No. 3, 1939, pp. 160-164.
2. Lilley, G.M. and Rainbird, W.J., "A Preliminary Report on the Design and Performance of Ducted Windmills," Rep. 102, April 1956, College of Aeronautics, Cranfield, England. Also available as Tech Rep. C/T 119, 1957, the Electrical Research Association, Leatherhead, England.
3. Igra, O., "Shrouds for Aerogenerator," Rep. No. 2, March 1975, Dept. of Mechanical Engineering, Ben Gurion University of Negev, Beersheva, Israel.
4. Foreman, K.M., Gilbert, B., and Oman, R.A., "Diffuser Augmentation of Wind Turbines," Solar Energy, Vol. 20, No. 4, April 1978, pp. 305-311.
5. Oman, R.A. and Foreman, K.M., "Advantages of the Diffuser Augmented Wind Turbine," Proceedings of the NSF-NASA Workshop on Wind Driven Generator Systems, Report NSF/RA/W-73-006, Dec. 1973, pp. 103-106.
6. Oman, R.A., Foreman, K.M., and Gilbert, B.L., "Investigation of Diffuser-Augmented Wind Turbines. Part II - Technical Report," ERDA Report C00-2616-2, Jan. 1977; also available as Research Department Report RE-534, Jan. 1977, Grumman Aerospace Corporation, Bethpage, N.Y.
7. Gilbert, B.L., Oman, R.A., and Foreman, K.M., "Fluid Dynamics of Diffuser Augmented Wind Turbines," Proceedings 12th Intersociety Energy Conversion Engineering Conference, Vol. 2, 1977, pp. 1651-1659.
8. Abbott, I.H., von Doenhoff, A.E., and Stivers, Jr., L.S., "Summary of Airfoil Data," Report No. 824, 1945, NACA, Washington, D.C.

9. North, P., "The Suppression of Flow Separation by Sequential Wall Jets," *Journal of Fluids Engineering, Transactions of the ASME, Series 1, Vol. 98, No. 9, Sept. 1976, pp. 447-452.*
10. Williams, B.R., "An Exact Test Case for the Plane Potential Flow About Two Adjacent Lifting Aerofoils," R & M 3717, Sept. 1971, Aeronautical Research Council, England.
11. Liebeck, R.H. and Ormsbee, A.I., "Optimization of Airfoils for Maximum Lift," *J. Aircraft, Vol. 7, No. 5, Sept./Oct. 1970, pp. 409-415.*
12. Eldridge, F.R., "Wind Machines," MTR-6971, NSF-RA-N-75-051, Oct. 1975, The Mitre Corp., McLean, VA.
13. Robbins, W.H. and Sholes, J.E., "ERDA/NASA 200 kW — Mod-OA Wind Turbine Program," Proceedings 3rd Wind Energy Workshop, Vol. 1, Sept. 1977, pp. 59-75.

## APPENDIX A

### DAWT ENGINEERING DESIGN

#### INTRODUCTION

This Appendix covers the engineering design activity for a prototype DAWT. Among the work tasks performed under the contract reported herein has been the design of a field test plan and an economic analysis of DAWT applications. Both of these objectives have required the conversion of the general lines and features of the baseline diffuser test model into an engineered structure. This prototype must be capable of safely withstanding the natural environment and remaining operational over a period of several years, as well as being produced, assembled, and installed in the field at reasonable cost.

The engineering design was initiated for the baseline diffuser configuration, which at the time had demonstrated an augmentation ratio of about 2.0 using screens to simulate turbine operation. In order to expedite the system design, the DAWT was configured around a modification of the Grumman Windstream 25 wind turbine system. This commercial product uses three untwisted, constant chord, extruded aluminum blades to power a 20 kW rated generator; maximum output is obtained in a 29 mph wind. The original blade diameter of 25 ft (7.5 m) was reduced to 18 ft (5.4 m) for DAWT application to reflect the then best current DAWT performance data, and to remain within the maximum output capability of the Windstream generator.

#### DESIGN CRITERIA

One of the problems encountered at the onset of diffuser engineered design was the lack of precedent and universal acceptance of the environmental exposure criteria for a structure of this type. Based on a review of Department of Commerce building design conference proceedings (Ref. A-1) and discussions with Rockwell Inc. personnel managing the Rocky Flats (CO) field test site for the DOE, the criteria for design of the diffuser shell were established.

We selected a 120 mph, sea level density wind as the maximum expected steady state condition for broadside (90 degree yaw angle) impact. A gust factor of 1.21 (Ref. A-1) was superimposed on the steady state condition to result in a maximum dynamic pressure of 53.7 psf applied at the DAWT centerline height of 30 ft (9.1 m) above ground level. The zero yaw angle condition also was considered but was found to impose a less severe structural loading condition than full broadside.

The diffuser shell structure was required to prevent permanent deformation under these wind loading conditions. Ice and snow loading were not specifically included for these considerations.

Because no comparable design had been attempted before, we established as an objective that the diffuser structure be capable of being manufactured by a sheet metal fabricator with a minimum of special tooling or process machinery. Also, the structure was assumed to be shipped to Rocky Flats, and erected there

without elaborate equipment. Because of the singular and prototype nature of the design, the material of construction was specified as being easily obtainable in standard, non-premium cost, sizes. Therefore, AISI 1025 carbon steel (36,000 psi yield strength) and standard commercial construction practices were assumed for the design. The assumption that this design was to be a field test article where ruggedness was a prime consideration and diffuser refinements were likely to be introduced at appropriate intervals during the field test program, led to a decision to use a safety factor of 4.0 for the initial point design.

The assumed circumferential loading on the diffuser was based on a modified theoretical cylindrical distribution equation valid under laminar flow field conditions. For circumferential angles,  $\theta$ , of up to 130 degrees on either side of the stagnation location, the local dynamic pressure  $q_1$ , was to be taken as

$$q_1 = q_0(1 - 4 \sin^2 \theta) .$$

In the angular position between 130 and 230 degrees the local dynamic pressure,  $q_1$ , was assumed constant at  $0.653 q_0$ .

As a result, the maximum local pressure at the top and bottom is found to be directed radially outward (i.e., suction) and to reach a peak value of three times the free wind  $q_0$ .

Subsequent wind tunnel tests, to be discussed in Appendix C, show in retrospect that the assumption for pressure distribution taken here was too severe, and that it penalized the field test article design.

#### PRELIMINARY FIELD TEST ARTICLE

The first engineering design of the DAWT, sized for the 18 ft (5.4 m) turbine, has a 18.7 ft (5.6 m) diffuser entrance diameter, a 30 ft (9.1 m) exit diameter, and an overall length of 13.3 ft (4 m) (see Fig. A-1). The initial boundary layer control annular slot has a height of 10.5 in. (27 cm) and the secondary annular slot is 3.0 in. (7.6 cm) high at an average diameter of 25.1 ft (7.5 m). The initial cylindrical section separating the turbine flow from the first slot flow is 4 ft (1.2 m) long, of which 2.4 ft (0.7 m) protrude upstream of the plane of rotation of the turbine. Figures A-1 and A-2 show that in addition to the three diffuser elements, a support structure and turntable constitute the assembly design.

While the diffuser sections generally are specified of AISI 1025 carbon steel, the compound curvature part of the major shroud element is designed of aluminum. Twenty-four steel longerons and interconnecting steel cables transmit the loads and shears of the diffuser sections' skin to the fore and aft main support rings. This truss work is bolted to the tubular support structure rising from a bearing support plate. The Rotek model A20-72P1A (Series 3000) gearless bearing is bolted at twenty-four equispaced places to a steel bed plate structure which is supported by the poured concrete foundation. The bearing can withstand a thrust loading of almost 1.5 million pounds and has a moment capacity of over 2.0 million ft pounds. The turbine centerline is 18.88 ft (5.67 m) above the foundation. A separate post support column is provided

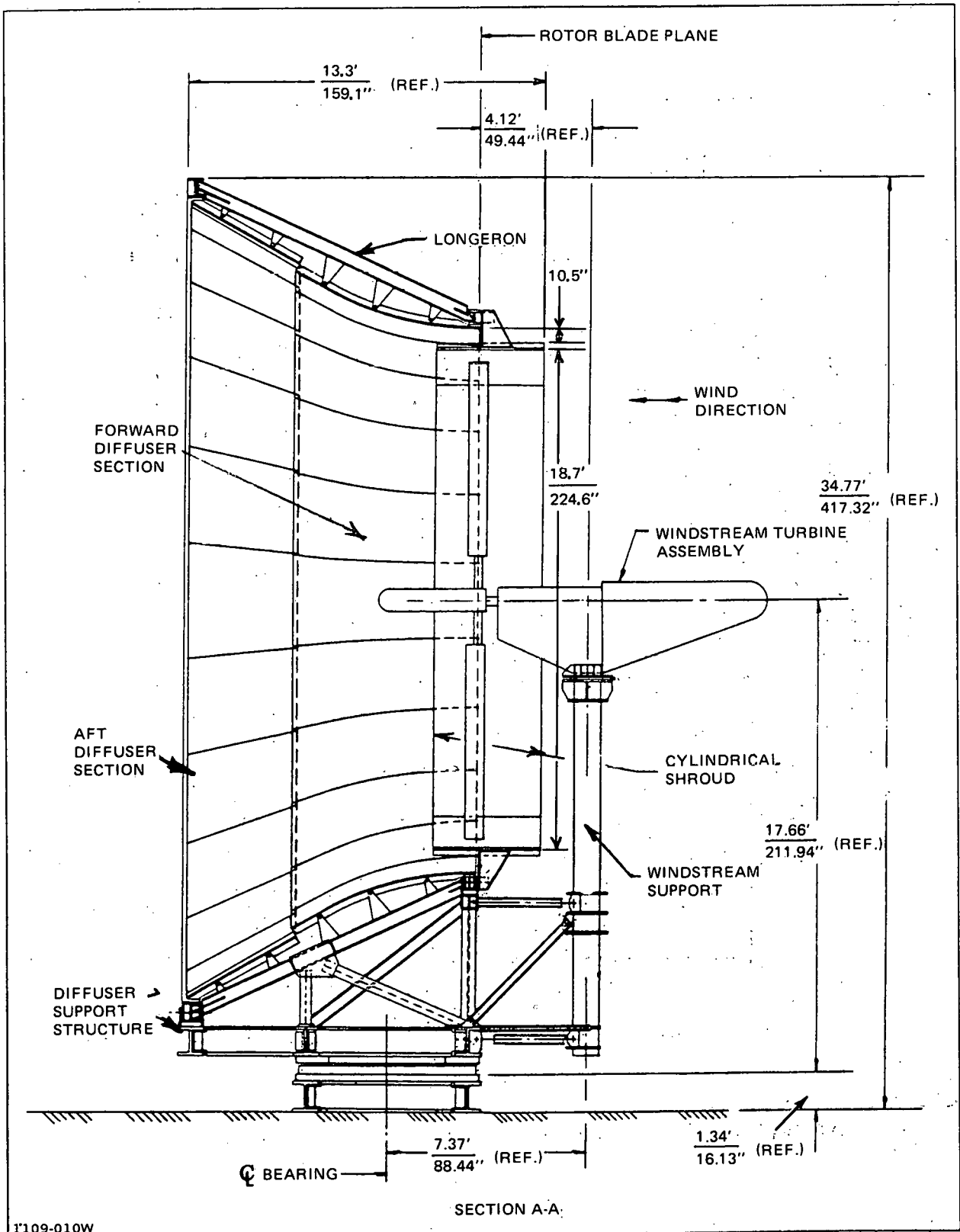


Fig. A-1 Engineering Design of DAWT Field Test Article – Side View. Thin, Formed Steel Skin; External Truss; Bolted Assembly; Roller Bearing Base



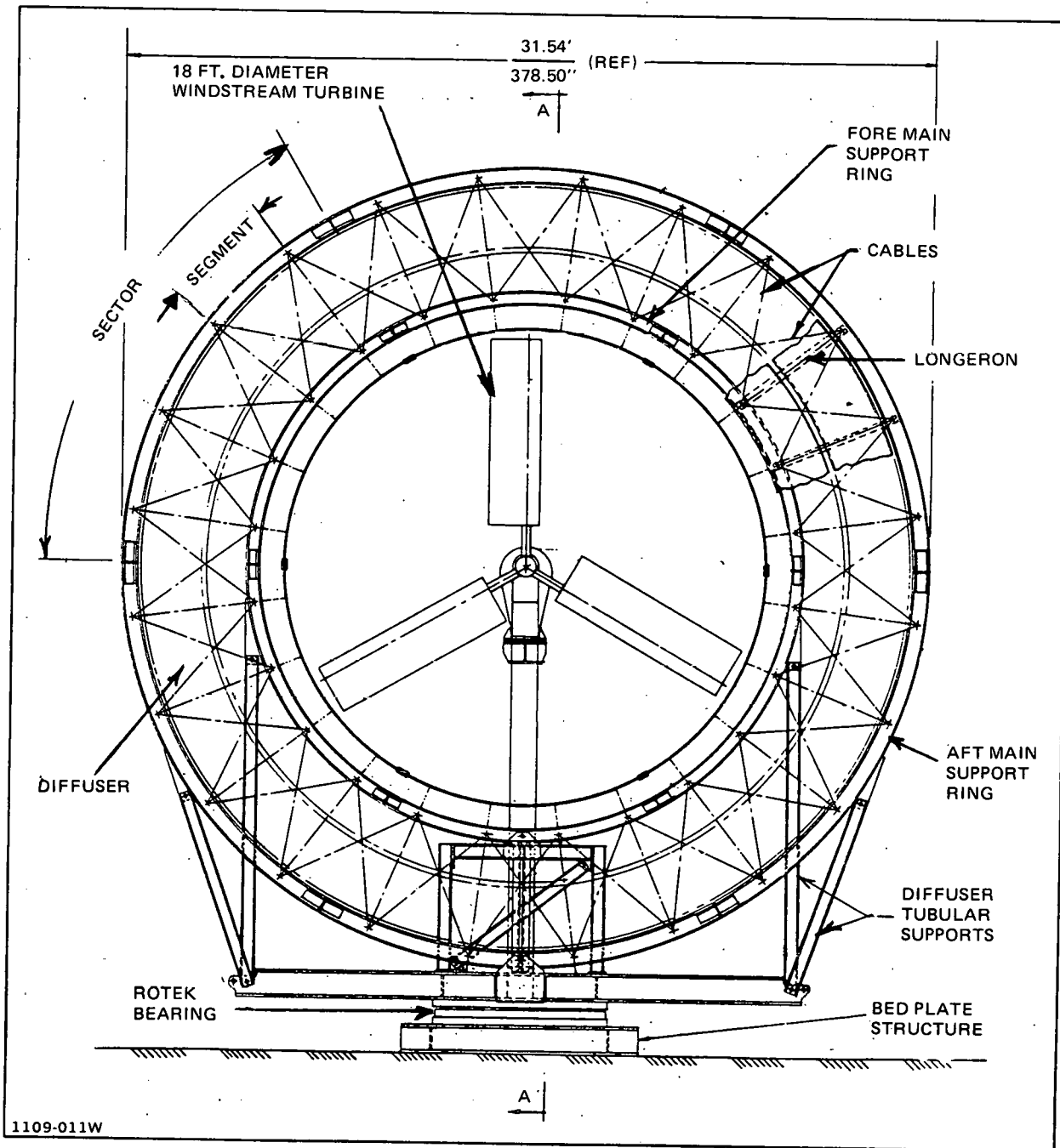


Fig. A-2 Engineering Design of DAWT Field Test Article – View Looking Forward (Upwind)

for the turbine subassembly so that tests independent of the diffuser can be conducted at the field site for comparative data.

The entire field test article is designed for bolted assembly in the field. However, the primary and secondary diffuser ducts can be partially preassembled into six sectors each. Each sector is made of four skin segments bolted together at flanges; the 48 in. (1.2 m) width of each segment has been dictated by the stock width of the most commercially available, least costly, sheet steel. An artist's rendition of this prototype field test article installed at the Rocky Flats site is shown in Fig. A-3.

An estimate of the weight, by major subassembly and overall, of the DAWT 18 prototype field test article is shown in Table A-1. Total cost projections for a single prototype assembled at Rocky Flats is shown in Table A-2. Three organizational cost estimates were obtained for the diffuser construction, assembly, shipment to and erection at Rocky Flats, the least of which amounted to about \$5.50/lb. Not included in this cost estimate were foundation and electrical connect costs. This one-off prototype design cost contrasts with the less than \$0.60/lb projection for production quantity manufacture based on recent Department of Commerce statistics for the type of product considered. Learning curve projections of 100th item cost estimates for this prototype field test article design cannot seriously be considered at this time for the following reasons:

- Production engineering redesign of the baseline diffuser for large quantity manufacture would take advantage of lower costs of improved manufacturing processes and methods, and mill quantity material size and cost procurement flexibility.
- A new engineering design approach for improved or substitute fabrication materials could drastically revise cost estimates of even a prototype baseline unit.
- Advanced diffuser configuration with better system performance than the baseline design could reduce diffuser size for given marketable rating, or upgrade a given size with a new rating, leading to another new engineering design effort and a new, revised prototype cost estimate.

#### BASELINE DIFFUSER REDESIGN

In the immediate period following completion of the initial prototype engineering design, there was a great temptation to exploit the three possible paths, noted above, toward diffuser design optimization in order to reach "bottom-line" energy cost values for a commercialized DAWT. However, because continuation of the planned diffuser development wind tunnel testing activity held a potentially greater impact for the long run than "cleaned up" baseline designs, we relegated only a minor follow-on effort from remaining contract funds to certain exploratory production-oriented redesigns of the prototype baseline DAWT. The areas of design investigation were:

- Various degrees of substitution of welded construction for the all-bolted initial design (see Figs. A-4 through A-8)

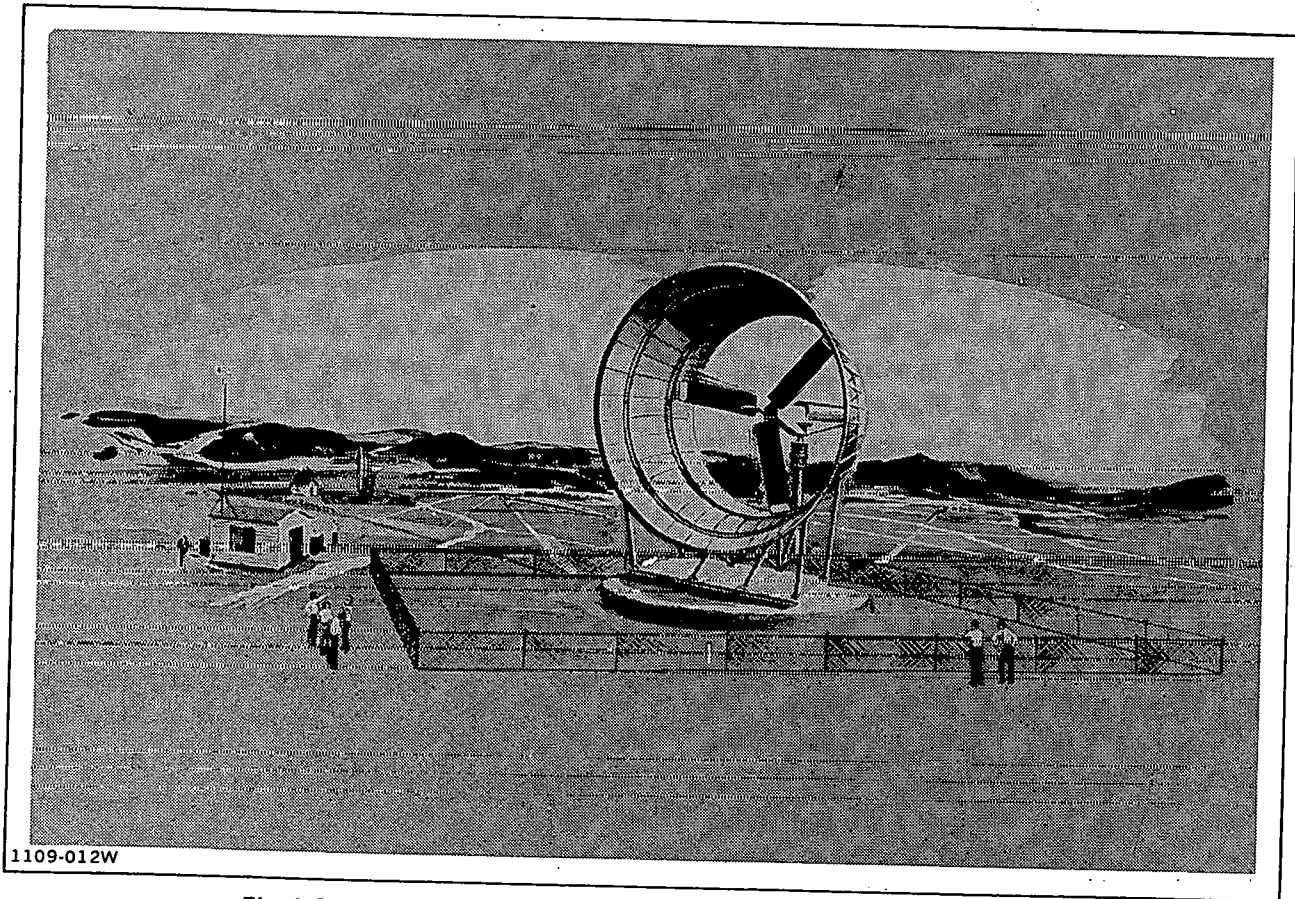


**Fig. A-3 Artist's Drawing of Baseline DAWT 18 Installed at Field Test Site**

**TABLE A-1 ESTIMATED WEIGHT AND RELATIVE COST FOR THE FIRST DAWT  
18 DESIGN STUDY**

DAWT Component	Estimated Weight (mild steel), lbs	% Total Weight (excluding turbine and foundation)	% Hardware Cost (excluding turbine, final assy, transp. and erection)
A. Diffuser assy	30,640	70	52 (exclusive of material cost)
1. 30 ft dia ring	4650	15.2	
2. 20 ft dia ring	2600	8.5	
3. 24 longerons	6912	22.6	
4. Aft ring panels (24), 1/2 in. steel	4380	14.3	
5. Forward cylindrical shroud, 3/16 in. steel	1930	6.3	
6. Double curvature panels, 3/16 in. thick aluminum	1450	4.7	
7. Panel splice tees (24)	1309	4.3	
8. Cables (24) and turnbuckles (48)	1872	6.1	
B. Diffuser support structure	11,980	2.7	
C. Wind turbine support structure	1313	3	24
Total DAWT (less turbine and foundation)	43,933	Raw Material and Purchased Parts 100%	24 100%
		Final Assy, Trans- portation (2000 miles) and erection	60% of hardware cost
		Total On-site cost	160% of hardware cost
1109-035W			

**TABLE A-2 DAWT COST PROJECTIONS (EXCLUDES  
FOUNDATION AND ELECTRICAL CONNECT  
COSTS)**

DIFFUSER & SUPPORT STRUCTURE (~45,000 LBS)		
• Prototype Estimates		
U.S. Steel (American Bridge)	\$250k	\$5.50/lb
Bath Iron Works	\$275k	\$6.10/lb
Grumman	\$590k	\$13.40/lb
• Grumman Windstream Wind Turbine (~2000 lbs)		
Production Cost ~ \$25,000		\$12.50/lb
• Production Cost Estimate (Department of Commerce Statistics)		
(2 - 3) x (Mtl Cost/lb) ≈ 0.40 - 0.60/lb:		
∴ Total Cost-Production Diffuser \$18 - \$27k		
1109-033W		

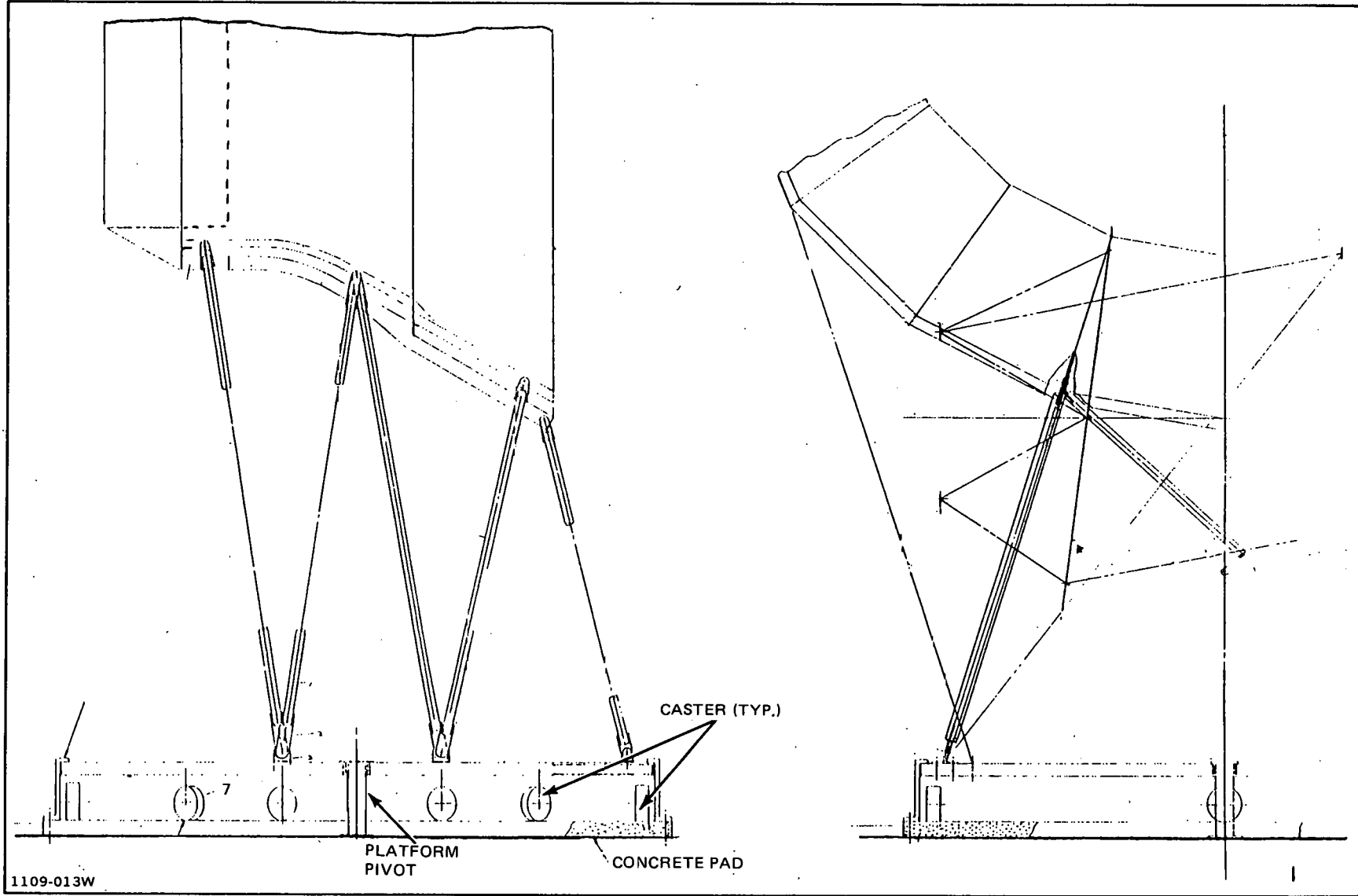
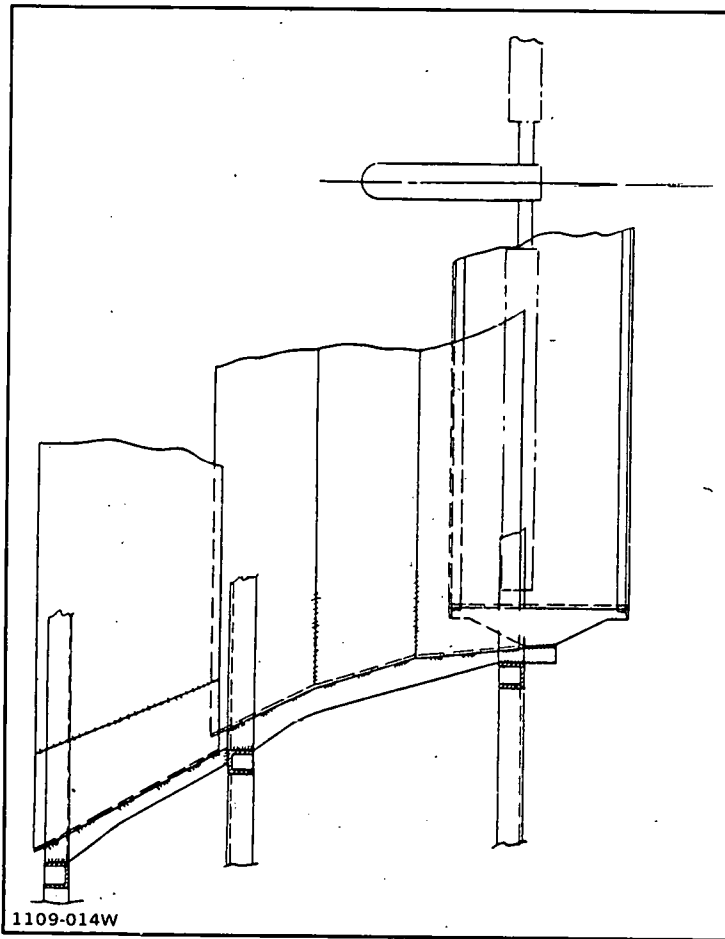
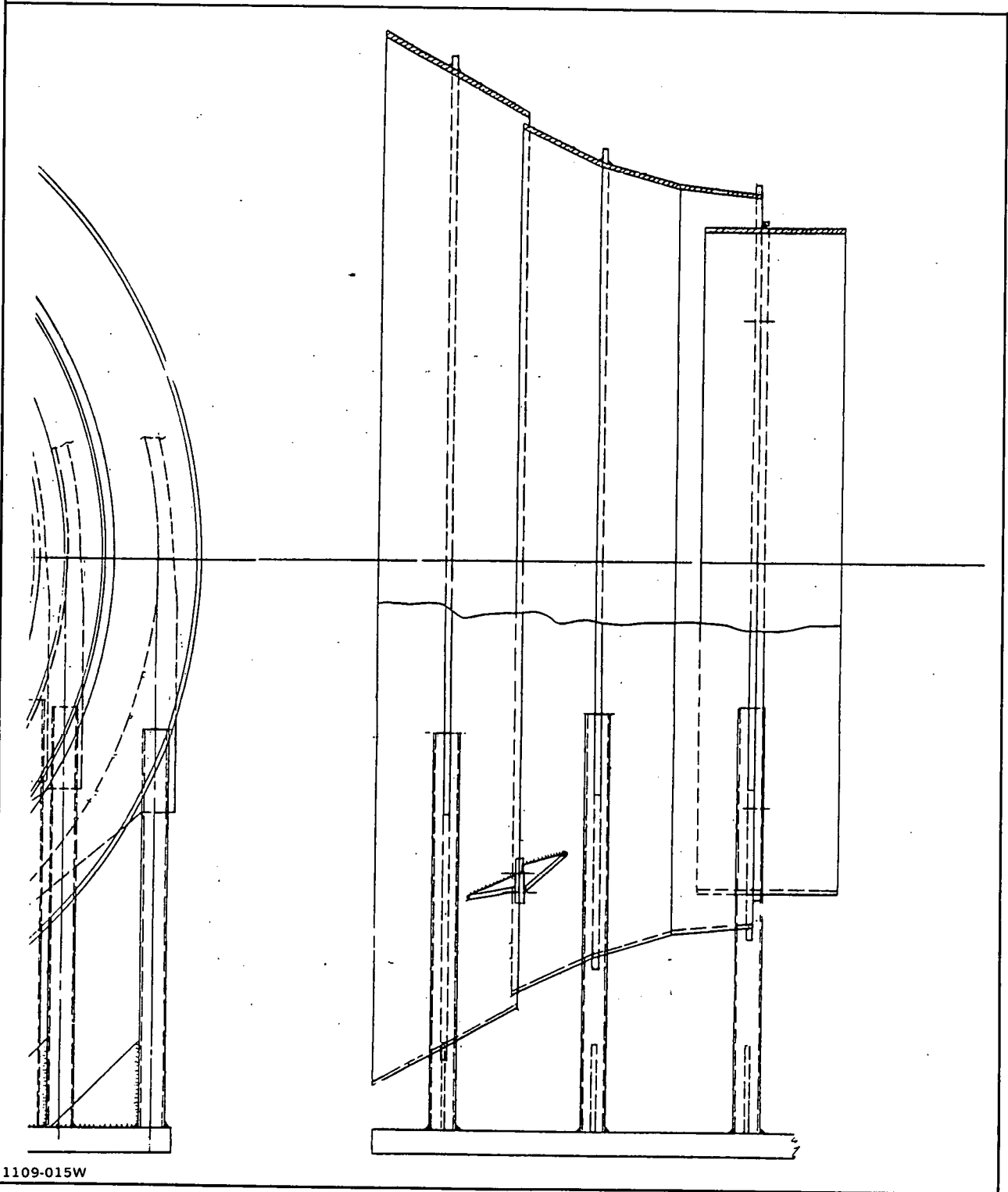


Fig. A-4 Alternate No. 1. Flat Thick Aluminum Plate, External Stiffeners, Welded Assembly, Center Pivot and Casters Base

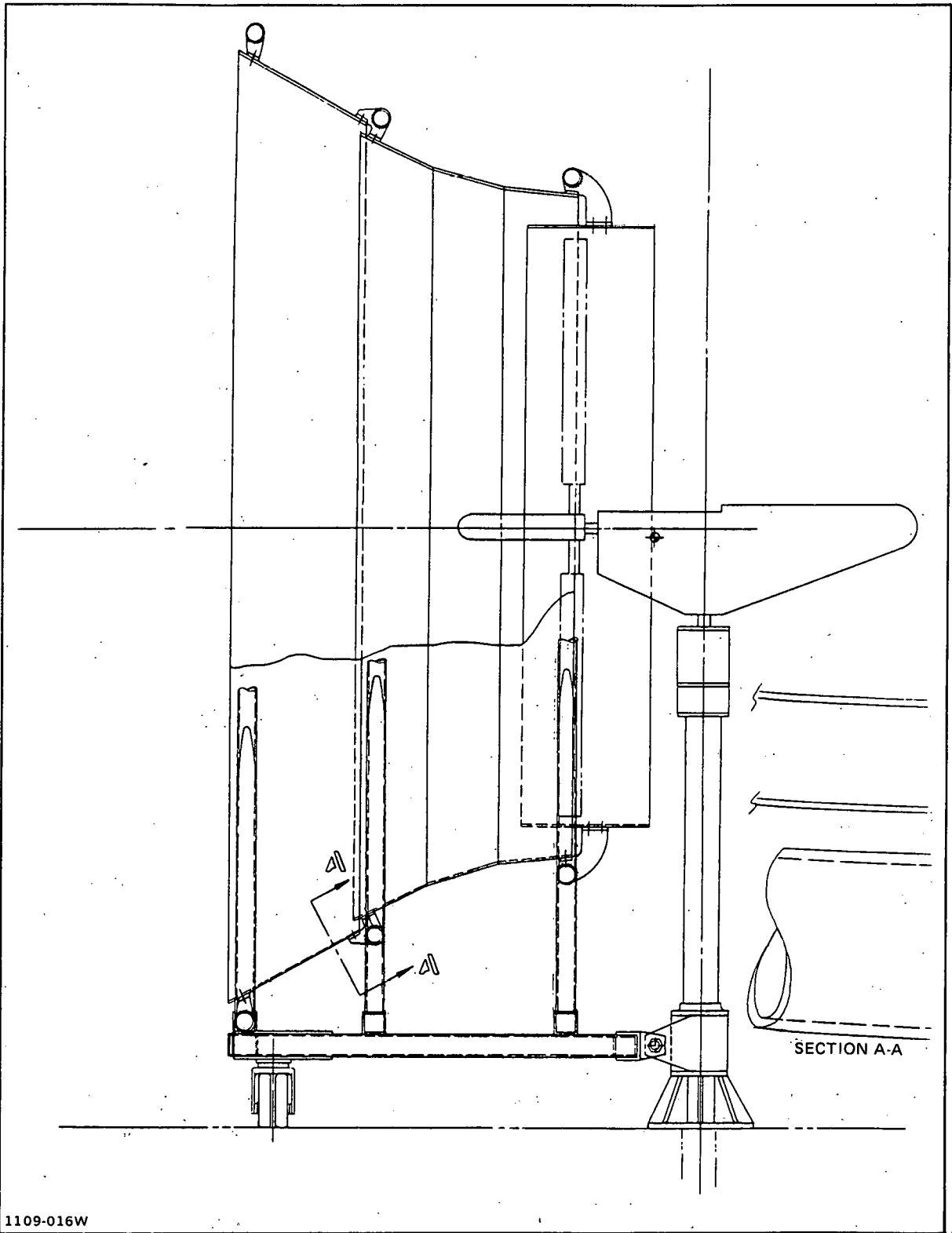


**Fig. A-5 Alternate No. 2. Flat Thin Rolled Sheet, External Stiffeners, Welded Assembly**



1109-015W

Fig. A-6 Alternate No. 3. Flat Thick Rolled Plate, No External Stiffening, Three Welded Segments, Bolted Assembly



1109-016W

Fig. A-7 Alternate No. 4. Flat Thin Rolled Sheet, Tubular Truss, Welded Assembly



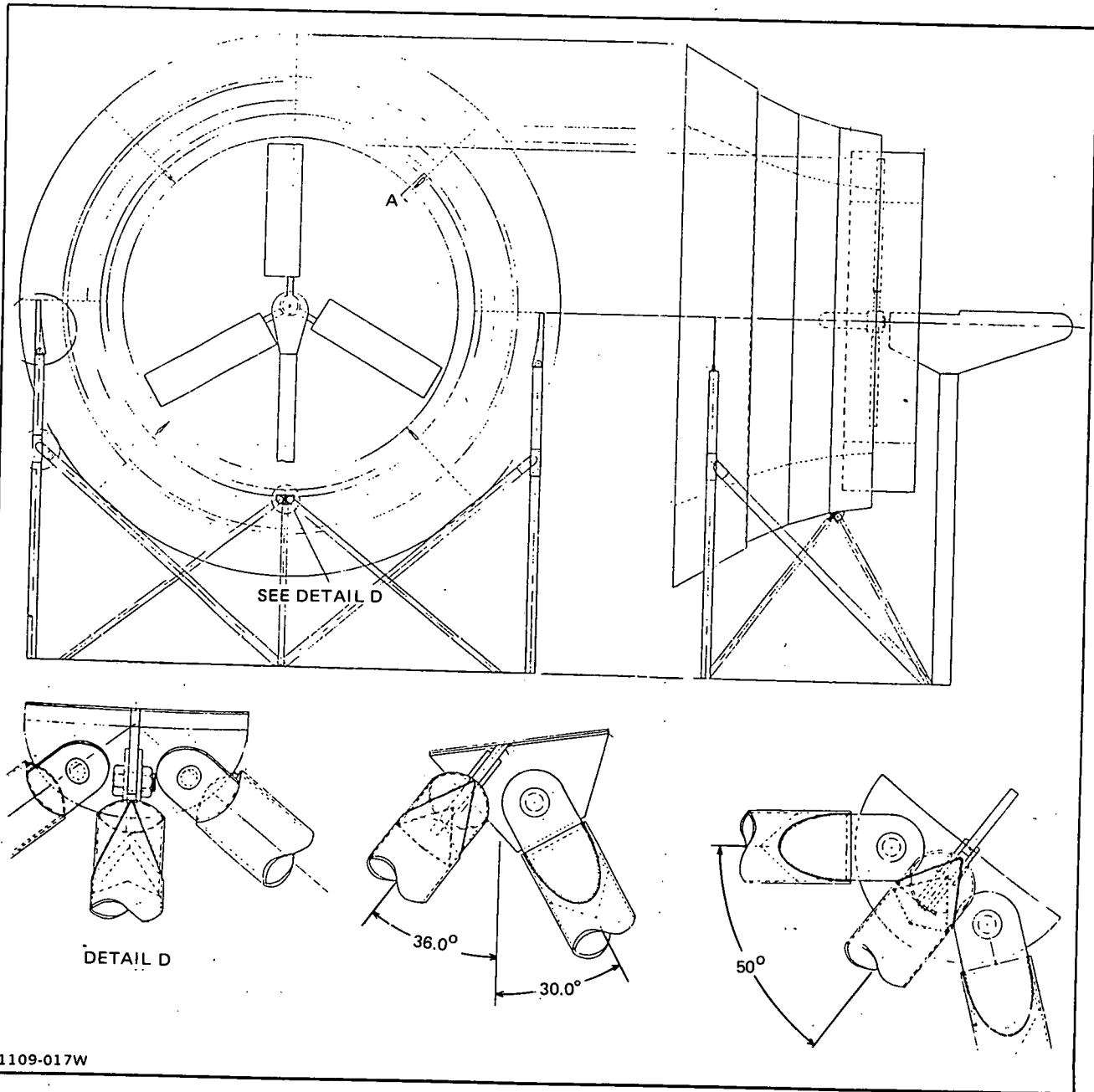


Fig. A-8 Baseline Design DAWT Thick Plate, Segmented Pattern, Cut from Rectangular Sheets, Bolted Support Structure

- Approximating the curved inner contour of the main diffuser section with various number of linear elements (see Figs. A-4 through A-8)
- Substituting an all-welded aluminum construction approach for the carbon steel material of the initial prototype DAWT (see Fig. A-7)
- Substituting a stressed skin structure for the lightly loaded skin, load-carrying truss, structural approach of the initial prototype DAWT (see Figs. A-6 and A-8)
- Substituting a center post and peripheral-mounted multiple caster approach, instead of the large base bearing assembly, to permit full azimuthal movement capability in response to wind direction changes (see Figs. A-4 and A-7).

Although time and budget precluded full economic assessments of all the re-design exercises, there were sufficient indications for designs of Figs. A-4 and A-8 to provide expectations of more improved economics than originally perceived possible.

In particular, a preliminary cost estimate for the welded aluminum baseline prototype diffuser (see Fig. A-4) reduces the sum of the direct and non-recurring construction costs to about 40 percent of the best estimate obtained for the initial bolted steel design approach. Use of aluminum and all-welded fabrication reduces the 20 ft diameter inlet diffuser assembly weight to about 2500 pounds (1134 kg) from the over 30,500 pounds (13,840 kg) weight for the steel version. Furthermore, this reduced weight allows the simpler and less expensive maypole with casters approach to be practical, instead of a weighty bearing assembly, at an estimated cost savings of over \$7000 for that function alone.

The design exercise represented by Fig. A-8 has an all-welded, carbon steel, stressed skin construction where the diffuser curved segments are pre-cut to pattern from rectangular plate. Elimination of the truss work of the initial prototype design reduces the diffuser weight by an estimated 7,600 pounds (3470 kg); at the lowest average cost per pound derived from the data on Table A-2, this offers a \$42,000 cost savings over the initial prototype manufacturing study.

Thus, while these exploratory studies do not present firm or detailed enough financial data to allow definitive decision-making, the significant cost cutting trends are clearly apparent. For this reason, we remain optimistic about probable costs of future optimized versions of the advanced DAWT energy conversion system.

## DESIGN ISSUES

In this section, we review the basic thinking that preceded the first design drawings. While this process has not been completely or rigidly followed in the designs generated to date, the incompleteness usually can be attributed to compromises in or a lack of opportunity to pursue specialized design information for potentially alternative approaches because of time and budget restrictions of the current contract. It is our expectation that further support

of this project investigation in the future will permit the full range of issues to be covered and lead to practical commercial products.

The principal issues accompanying the establishment of a cost-competitive DAWT system are

- Size or rating of unit
- Structural design criteria
- Material selection
- Operational and environmental factors
- Manufacturing approach
- Economics of geometric size and production scale
- Siting characteristics.

These issues are, to a large extent, closely interrelated, and what follows is intended to provide guidance discussion, rather than a detailed description for system analysts of similar problems.

#### SIZE ISSUE

From the basic wind power equation, the power rating is related to the second power of turbine diameter. In addition to this relation to physical size, the power rating of a DAWT system will be dictated by the perceived high sales market for different DAWT ratings.

With regard to turbine size, we see two basic approaches possible at this time. The first can be characterized as a low cost, extruded blade technology approach. This design features an untwisted, constant chord, constant cross section for the entire length of the rotor. Pitch variation of the blade is made possible by a rotation mechanism at the root, or hub, of the rotor assembly. Optimized aerodynamic performance of each blade is sacrificed in the interest of cost savings in design and manufacturing. But this low cost extruded rotor is limited in span size (i.e., rotor diameter) because of aeroelastic loading effects on the cantilevered method of attachment for a given cross-sectional size. Limitations on maximum cross-sectional size are imposed by the available extrusion press machinery capacity.

Larger sized turbines can be constructed by the second approach consisting of a combination of spars and outer skins assembled together, in a manner similar to aircraft wing practices, by riveting or welding. Variable cross-section dimensions and shape, as well as span-varying twist, are possible with this construction procedure. The cost of this complexity presumably is justified by the degree of aerodynamic performance improvement made possible along the rotor blade span. This second approach currently appears economically attractive and unchallenged for ratings of about 100 kW or greater. However, despite the design complexity accepted for this approach, a practical span size limitation comes into being when the incremental cost of larger span rotors increases at a faster rate than the accompanying increment in power conversion.

This inordinate rise of blade cost-to-benefit ratio is brought about by the need to overcome or overdesign for the aeroelastic loading of very long, slender, cantilevered blades (Ref. 6).

Recent developments with filament wound, bonded fiberglass blades hold promise of extending the size of rotors well beyond that of all-metal blades. However, this technology currently is far from operational in blade spans on the order of 150 ft (46 m), and good production cost data are unavailable (Ref. A-2).

The maximum practical cantilevered blade span for the low cost blade technology is considered between 15 and 18 ft (4.6 to 5.4 m). Such blade designs are utilized in the Grumman Windstream 25 system. At a rated speed of 20 mph (32 kph), and equipped with a 30 ft diameter rotor, the commercialized DAWT power rating could be in the 40 to 70 kW range corresponding to DAWT model test performance indicating the likelihood of at least 4, and up to 7 times the power coefficient of conventional wind turbines.

Of additional significance is the benefit to be derived in capacity factor of the DAWT relative to a conventional wind turbine. Table A-3 compares the plant factors of both systems using the approximate Justus linearized equation for average wind variance (Ref. A-3). Various site average velocities,  $\bar{V}$ , between 9 and 18 mph (4 to 8 m/s) are examined for the cut-in and rated velocities,  $V_i$  and  $V_R$  respectively, of the conventional Windstream and the projected values for two baseline DAWT designs. It is evident that because the diffuser produces a local increase in air speed over free wind conditions, depending on the magnitude of augmentation ratio, the DAWT's turbine can be operated at its rated power more often than a conventional turbine. For the lowest average site wind speed, the DAWT has about one-third more capacity factor than a conventional (Windstream type) WECS. For the same rated wind speed, this DAWT capacity factor advantage increases as the site average wind speed decreases. However, the annual energy production of the DAWT is the product of the capacity factor and the augmentation ratio, and for the examples of Table A-3 results in four to eleven times more annual energy than the Windstream type conventional WECS system.

TABLE A-3 PLANT CAPACITY FACTOR CALCULATIONS (RATED  $V = 8.9 \text{ M/S } (\sim 20.0 \text{ MPH})$ )

Site Avg. Wind Velocity		DAWT		Windstream Type WECS (%)
		Baseline Diffuser (%)	Advanced Diffuser (%)	
m/s	(mph)			
4	(8.9)	25	27	17
5	(11.2)	36	37	28.5
6	(13.4)	46	47	40
8	(17.9)	66	67	62
Major Design Parameters		Aug. Ratio = 4 $V_i = 22 \text{ m/s } (5 \text{ mph})$	Aug. Ratio = 7 $V_i = 1.9 \text{ m/s } (4.3 \text{ mph})$	Aug. Ratio = 1.0 $V_i = 3.6 \text{ m/s } (8 \text{ mph})$
1109-036W				

For the built-up metal construction and epoxy bonded filament-wound blade technology the diffuser provides an opportunity for minimizing blade design and manufacturing complexity and cost for large, multi-MW-rated systems. Although no new economic analyses for large systems have been conducted under this present contract, prior work (Ref. 6) indicated a favorable crossover point for the DAWT at a WECS rotor diameter of about 120 ft (40 m). Depending on the outcome of currently DOE programmed cost reduction programs for large rotors, the large size DAWT applications scenario requires a future analysis update.

#### STRUCTURAL DESIGN CRITERIA

Diffuser design to date has been predicted on a limiting elastic deformation criterion under assumed maximum wind conditions. In an earlier part of this section of the report, the assumed pressure distribution on the diffuser was described. Low Reynolds number wind tunnel data also are reported herein (see Appendix C) showing that the design assumptions were, perhaps, too severe, thus leading to ultraconservative, economically penalized designs. The most severe wind loading condition on the diffuser is for a yaw angle of 90 degrees. Despite the conical frustrum shape of the diffuser, and partial porosity because of boundary layer control slots, the shape behaves as a circular cylinder to side wind orientation judging from wind tunnel test model data. At an intermediate Reynolds number between  $10^4$  and  $10^5$ , the aerodynamically clean small scale models exhibit an overall drag coefficient of 1.15 (at 90 degree yaw) compared to accepted values of 1.2 for circular cylinders.

In the real world of commercialized DAWT, characterized by a) large diffuser size, b) maximum wind speed of the installation environment, and c) widely dispersed external roughness elements necessitated by engineering construction features for the diffuser, the Reynolds number will be in the fully turbulent region and the overall drag coefficient for 90 degree yaw wind should drop to approximately 0.30. With this lower drag loading, the pressure distribution over the diffuser should change from the results obtained from wind tunnel model testing, and this will affect the structural loading criteria. Within the constraints of readily available wind tunnel facilities, as previously described, these operational factors can only be simulated; field tests ultimately must provide the detailed information, and until these data are obtained, DAWT diffuser structures most likely will be overdesigned.

A second element involved in the structural design criteria is the safety factor used in the detailed design analysis. The safety factor of four applied to the initial DAWT prototype design, previously described, is much larger than the 1.5 to 2.0 safety factor conventionally used in aerospace structures. While the larger value may be justified because of 30-year lifetime requirements, commercial fabrication practices, and expectations of low maintenance availability, clearly, much better information and rationalization is needed to preclude too severe an economic penalty on a DAWT structure.

The deflection criterion of 1.5 percent of radius allowed locally in the cylindrical section surrounding the turbine should be adequate to prevent turbine blade interference. This local constraint to assure trouble-free operation should not be critical to overall diffuser design because local stiffening can provide a viable solution.

## MATERIAL SELECTION

This issue impacts directly on the design and manufacturing approaches that will be taken, and on the ultimate cost of the structure. At least three options tentatively appear attractive:

- A steel or aluminum structure
- A fiberglass sandwich structure
- A ferrocement structure.

Metal and fiberglass sandwich parts can be made in a factory where production scale economics and quality control can be exercised easily. The parts can be joined into a DAWT subassembly except that this approach increases the bulk and value of the transportable material to the installation site. Greater handling care and parts protection in transit adds to overall costs and offsets partly the production economies. Erection and assembly at the installation site necessitates heavier handling capacity and more expensive capital equipment for large subassemblies in contrast to the greater assembly labor burden where components are fitted together in the field.

Steel construction is relatively low in material cost but has the drawback of higher weight and handling cost for large assemblies compared to aluminum. Steel also incurs a greater life cycle cost because of requirements for periodic environmental protection. The availability of very high strength and corrosion resistant specialty alloys increases the versatility of design which must be traded off against the higher cost of these steels. While an extremely large number of experienced fabricators of ordinary steel products exists in the U.S., the numbers are markedly reduced for those competent enough to fabricate specialty steels.

Aluminum has become a widely used construction material in the U.S. that suffers from high initial material costs but offers lower life cycle costs than steel. In stressed skin designs requiring a large section modulus, aluminum leads to lighter and less expensive designs than steel of comparable yield strength.

Fiberglass sandwich construction also has high initial material cost but requires relatively low capital investment in machinery and tools. Thus, fiberglass sandwich construction is compatible with the requirements for easily changed design construction during a progressive or rapidly evolving development cycle. This material can be molded into subassemblies with excellent surfaces finish, esthetic appearance, and low life cycle costs. Relative lightweight means reduced shipping costs, as well as on-site erection and assembly costs, although greater care and protection is needed for transporting the fiberglass than metal subassemblies. Variable section thickness is easily accommodated with fiberglass construction, where designs can benefit from this feature. Field repairs of a minor nature can be made to fiberglass sandwich structures although major damage can best be overcome by replacement. Sufficient numbers of competent fabricators of large fiberglass sandwich units exist in the U.S. to support a DAWT industry.

Ferrocement has the great attraction of being a very cheap raw material. Maintenance costs also are low, although ferrocement results in heavy weight. Complete DAWT structures may be constructed of ferrocement subassemblies made in factories, or constructed completely at the installation site. For the latter, a great deal of labor is required applying the cement to the steel screen mesh form erected in the field. This labor, however, need not be as skilled or as costly as structural metal fabricators according to experienced contacts. Modular ferrocement subassemblies can be made in factories with quantity production economies and completed as an integral assembly in the field. However, the latter step will require heavy capacity handling equipment. Tooling and machinery costs are low for both field or factory fabrication with ferrocement compared to metal fabrication. Another advantage of this material is that complex curvature of internal flow passages can easily be reproduced, and low maintenance, esthetic appearance, and easy repair are characteristic. From discussions with former U.S. Navy project officers in charge of ferrocement development projects, a major barrier to ferrocement use appears to be the very few experienced manufacturers in the U.S., and the small number of experienced designers and cost estimators that could work on DAWT commercialization ventures. However, a heavy commercial demand for ferrocement structures could stimulate innovative automated manufacturing methods that would have the effect of reducing drastically the labor-intensive mortaring skills now required. Increased use of this material probably would lead to the organizing of training programs in order to provide the labor pool needed at all skill levels.

#### OPERATIONAL FACTORS

In contrast to the high performance sensitivity of conventional horizontal axis turbines to wind vector yaw, DAWTs are virtually unaffected by off-axis wind directionality of up to 30 degrees, according to test data (Ref. A-4). The relatively large surface area of the diffuser can provide large yaw forces with off-axis winds, but the diffuser mass resists rapid automatic weather-cocking at low wind speeds. At high wind speeds and high gustiness, the yaw forces can become large enough so that some damping of horizontal rotational tendency may be desirable. Placement of the center of DAWT rotation has to be a compromise between the turning moment at the high and low wind speeds, and the gyroscopic loading on the turbine blades. Lighter diffusers, because of material and design decisions, will have reduced effectiveness in controlling response to sudden yaw forces. However, smaller diffusers, while lighter in overall weight will have reduced yaw forces acting on them.

While the DAWT requires a built-in wind yaw following capability, it need track only relatively long persistence wind field changes and at a moderate rate of rotational change. An active controller appears suggested whereby constant yaw change rate to within 10 to 15 degrees of overall free wind direction is provided for any wind speed in the operational range.

To prevent excessive loads on the turbine blades, an operational requirement is to be able to shut-down the DAWT at very high, hurricane level wind speeds. Blade feathering and intentional misalignment of the diffuser are some measures to produce power shutdown. In addition, a positive locking system should prevent rotor operation during periods of maintenance or inspection.

## ENVIRONMENTAL FACTORS

The main natural environmental extremes that must be considered are ice, snow, windborne sand and gravel, and seasonal extremes of temperature. For steady and moderate-to-high winds, the internal flow in the diffuser and rotating blade wake made it unlikely that major snow or ice buildups will take place on the critical-diffuser components. At low wind speeds and heavy snowfalls or icing, the DAWT's yaw rotational capability could become immobilized. One of the possible solutions is a protected race, or bearing surface on the ground to prevent intrusion by snow and ice.

Sandstorm erosion is a potential problem that could affect the life cycle costs of metallic or fiberglass constructed diffusers. The elevation of the DAWT installation should exclude most of the likely high concentrations of large solids impacting the diffusers; however, the foundation and supports may need some barrier protection.

Temperature extremes can affect the clearance between the rotor and diffuser shell, but pose no unique design condition that has not already been experienced in many commercial structures. Expansion joints may have to be provided, depending on material selection and design.

Human factors affecting the DAWT design are esthetics, public safety, equipment security, and interference with communications links. The continuous and static structure of the diffuser lends itself to creative design or decoration and pleasing appearance and enhanced safety for maintenance people, as well as the general public and wildlife.

## MANUFACTURING ISSUE

This issue must be evaluated by its impact on the ultimate cost to the energy user. Some of its variables concern technology applied to direct manufacturing procedures; physical size of the DAWT; the location and accessibility of potential user sites to final assembly, installation, and maintenance crews; the proximity of the manufacturing site to the ultimate installation sites; the availability and cost of fabrication materials; the supply and productivity characteristics of the labor pool available to the fabrication plant; and the restrictions on routing, distance, and size of load imposed by shipping links. Clearly, this issue interacts also with the design, sizing, and siting aspects of the DAWT project.

Primary metal-working machinery and fixtures are designed to handle standard commercial sizes of sheet or coil steel or aluminum. Secondary operations, such as joining of components into major subassemblies, or full assembly, are limited to sizes compatible with interstate trucking or other shipping modes linking the production facilities to the installation site. Transport of fiberglass subassemblies also has to be compatible with shipping mode restrictions. However, primary manufacturing operations are somewhat less inhibited by size for fiberglass than for metal. Ferrocement has, perhaps, the greatest flexibility for on-site construction because bags of cement and rolls of steel screen are easily transportable by bulk interstate carriers. Factory-made ferrocement parts have inherent size and weight barriers in ease of ship-



ment and this may result in a larger number of transportation units than other materials to complete (e.g., a large DAWT). However, better quality control can be maintained in a factory environment than at a field site.

With this brief review of the more obvious aspects of material selection impacting on the manufacturing issue, one may conclude that economic tradeoff studies are necessary. However, a practical index also is needed to evaluate the tradeoffs; one recommended index is the total DAWT capital cost.

Total manufacturing cost, affected as it is by the direct cost of labor material, machinery, special tools and fixtures, and shipping, will be sensitive to the basic design approach relative to labor intensity vs. automated machinery operations and the construction material selected. To a lesser extent, alternatives offered by regional and skills differentials in labor cost must be incorporated in early thinking. And because DAWT physical size interacts with machinery capabilities and the traditional experience of different labor pools, it is probable that no universally applicable approach may exist across the complete DAWT marketing spectrum; different DAWT rating classes must be examined for production cost elasticity in existing, as well as new, manufacturing facilities.

We identify, then, at least four possible degrees of alternative action that should be considered in judging the manufacturing issue against a cost index:

- 1) For a particular construction material, emphasize simplified or automated processes instead of high skill, labor intensive operations.
- 2) Use higher cost but higher strength materials to reduce component and assembly weight and improve manufacturing, handling ability, and field installation.
- 3) Use low cost materials in processes needing relatively unskilled employees.
- 4) Reduce plant overhead costs and finished product shipping mode costs by moving production labor and raw materials from one installation site to another, similar to road building, instead of parts from the factory to the installation site.

#### PRODUCTIVITY ECONOMICS

It is a matter of record that production of large numbers of identical articles generally has lower unit labor cost than the identical initial prototype item. Two major factors usually determine the labor cost. The first category includes hourly wages, fringe benefits, payroll taxes and workman's insurance, etc., and generally does not vary with production rate or total quantity (Ref. A-5). This category of cost is inherently included in cost estimates for a prototype design. The second factor relates to the amount of work that personnel can accomplish in a finite time period, or productivity. Affecting labor productivity are such elements as working environment, regional variations in labor training, general experience, skills, and work schedules, management capability and philosophy, and, finally, the improvement in per-

forming tasks that results from practice and the accumulated experience of repeated operations (Ref. A-5). This last element is called the learning or experience curve which can be expressed in the form

$$y = ax^{-b}$$

where  $y$  = index of cost per unit product

$x$  = cumulative units of output

$a$  = theoretical cost of the first unit of production

$b$  = index of rate of decrease of labor for multiple units of production

The learning curve is more usually characterized by the progress index, PI, as the percent reduction in labor cost for each doubling of output, or

$$PI = 2^{-b}$$

(A "PI" of 80 percent, meaning that labor costs are lowered to 80 percent of the prior value when output is doubled, yields a "b" parameter of 0.322).

Although some controversy had been connected with the learning curve model when it first was advanced, objective empirical investigations (Ref. A-6) clearly prove the relevance of this concept in a wide spectrum of labor intensive manufacturing and construction industries (Ref. A-7). However, what has also been indicated by these studies is that at some point in the learning curve, a steady state phase may be encountered. However, this interruption of the learning curve, which results in essentially constant labor cost with further output increases, cannot be predicted for any given industry or quantity of production, but must be detected from direct production experience. Furthermore, the evidence is that PI values vary greatly in different industries, and that a single universal average value probably is invalid (Ref. A-6). Information available for uninterrupted construction industry activities (Ref. A-7) indicates PI values varying between 80 and 95 percent (see Table A-4). In our opinion, an appropriate and reasonable preliminary average PI value for DAWT production, either in the metal, fiberglass, or ferrocement version, is 90%. Therefore, the expected labor hours and cost of the tenth and hundredth units should be about 70 and 50 percent, respectively, of the identical prototype unit. Projections beyond the hundredth unit are too uncertain at this time because of the unpredictable nature of the onset of the steady state phase.

The other elements of labor productivity are not easily quantified for design cost estimation and are beyond the scope of this present discussion.

#### SCALE ECONOMIES

There are two types of scale economies possible to interact with commercialized DAWT costs. The first type results from production numbers and the second is associated with unit size or rating.

**TABLE A-4 DECREMENTAL CONSTANTS FOR  
CONSTRUCTION ACTIVITIES**

(FROM Ref. A-7)

Activity Description	PI (%)
Entire structure of ordinary complexity such as high-rise office buildings and tract housing	95
Individual construction elements requiring many operations to complete such as carpentry, electrical work, plumbing, erection and fastening of structural units, concreting	90
Individual construction elements requiring few operations to complete such as masonry, floor and ceiling tile, painting	85
Construction elements requiring few operations on assembly-line basis such as field fabrication of trusses, formwork panels and bar bending	80
Plant manufacture of building elements such as doors, windows, kitchen cabinets, and pre-fabricated concrete panels	90 - 95
1109-034W	

In addition to the expected economic benefits obtained with large quantity production through learning curve effects on reducing cost per unit (i.e., increased productivity), there are economies to be realized from the scale of operations. The latter savings come about from 1) an ability to command larger quantity discounts from large purchases of basic construction material, 2) greater operating efficiency resulting from the planning and marshalling of resources and manufacturing equipment for long production runs, and 3) the spread of indirect and preparatory expenses over a larger number of produced articles, thereby reducing the burden on each unit product.

The size, or output rating, of the DAWT is a system capacity scaling that can affect costs of production in two ways. The first aspect affects the ability to purchase standard components such as generators, transmissions and bearings, at low cost because of widespread commercial use and already existing high production rate economies which depress unit sales price. The second aspect results from the elapsed time necessary to complete a single operating system on site, and the maintenance of inventory to provide market service. This aspect affects overall manufacturing costs by virtue of the loss of earning power of tied up financial resources. Large DAWT units with nonstandardized ratings for purchased components, probably impose the most cost-of-money burden for life-cycle economic evaluations. On the other hand, creation of a new (i.e., non-standard) rating class with the potential for large quantity production because of market demand, could eliminate the burden of high purchasing cost and large inventory carrying charges. However, at this stage of the DAWT project we are unable to predict what a currently non-standard component would cost if it were suddenly to be required in extraordinarily large numbers.

The mission study reported in Ref. A-8 suggests two prime applications sectors for wind energy that, if fully developed, would have large enough numbers to establish a standard market rating posture in its own right.

These two markets are for 1) single-family residences of about 10 kW unit rating with sales potential of over nine million units, and 2) farms and farm production of about 40 kW unit rating and a sales potential of over three quarters of a million units.

For a 30 year lifetime, the potential of market demand growth, although full of uncertainty, must nevertheless be considered. Therefore, the customer's investment cost in a unit of capacity size to meet likely future demand must be compared to the total life cycle cost of meeting only current demand initially and adding to or replacing the in-place DAWT with another unit some time in the future at inflation-driven higher unit cost. These considerations obviously will interact with the sizing and manufacturing issues; updated market scale identification which differs from the referenced mission study (Ref. A-8) can also influence these considerations.

#### SITING ISSUE

The major aspects of this issue relate to:

- Wind characteristics.
- Accessibility for installation and maintenance
- Proximity to and nature of the market for the DAWT's output
- Weather environment.

We have touched on all of these items in prior discussions of the sizing design and manufacturing issues. For example, in computing the DAWT plant capacity factor we confirmed the general observation about WECS that high average wind speed locations are particularly useful for WECS rated at a high wind speed. It also follows that high average wind speed sites could be attractive for large rated output systems, such as might be erected by utilities. Therefore, it becomes important to identify the characteristics and proximity of the energy market for the DAWT's output. Long transmission lines, if needed to integrate large DAWT's into utilities, may partially offset the economic benefits of megawatt size units at high average wind sites.

However, if the 40-100 kW demand market is close to the high wind speed location, then this lower rating may prove most economical. So, it is not obvious without complete economic considerations of the market for power as to the best DAWT size assignment for high wind energy potential sites.

At the other extreme, because of the enhanced energy conversion capability of DAWT, what might seem like marginal potential sites for conventional WECS may prove applicable to intermediate sized DAWTs.

The ruggedness of terrain, in addition to increasing the cost of site preparation and DAWT installation procedures, also will affect the variation of windspeed with height. The former effect cannot be predicted a priori in this present study, but has to be considered as an incremental cost burden which must be offset by the particular attractiveness of the real estate,

market proximity, or high cost of energy alternatives. In unique wind situations at some sites, the channelling of flow may preclude the need for DAWT directional change mechanisms and the resulting cost savings could become a special site application bonus.

#### REFERENCES

- A-1 Koppes, W., "Design Wind loads for Building Wall Elements," - in Proc. NBS Building Science Series 30, November 1970, pp. 9-18.
- A-2 Sullivan, T.L., Cahill, T.D., Griffee, Jr., D.G., and Gewehr, H.W., "Wind Turbine Generator Rotor Blade Concepts with Low Cost Potential," DOE/NASA/1028-77-13, NASA TM-73835, December 1977.
- A-3 Justus, C.G., et al., "Reference Wing Speed Distributions and Height Profiles for Wind Turbine Design and Performance Evaluation Applications," ERDA Report ORO/5108-76/4, August 1976, p. 41.
- A-4 Igra, O., Shrouds for Aerogenerator, Rep. No. 2, Dept. of Mechanical Engineering, Ben Gurion University of the Negev, Beersheva, Israel, March 1975.
- A-5 Paulson, B.G. , Jr. "Estimation and Control of Construction Labor Costs," J. Const. Div., Proc. ASCE, Vol. 101, No. C03, September 1975, pp. 623-633.
- A-6 Baloff, N., "Extension of the Learning Curve - Some Empirical Results," Op. Res. Quart., Vol. 22. No. 4, December 1971, pp. 329-340.
- A-7 Gates, M. and Scarpa, A., "Learning and Experience Curves," J. Const. Div., Proc. ASCE, Vol. 98, No. C0-1, March 1972, pp. 79-101.
- A-8 Garate, J.A., "Wind Energy Mission Analysis, Final Report," ERDA Report C00/2578-1/2, General Electric Co., Space Division, Philadelphia, PA, February 18, 1977.

## APPENDIX B

### DAWT BUSBAR COST OF ENERGY

To indicate the prospects for commercialized DAWT with some degree of design/manufacturing optimization, we will develop here the possible busbar cost of energy using a DAWT system.

As a point of departure, we examine the detailed design and data developed for a field test article and presented at a Design Review on February 16, 1978. This design employs an 18-foot diameter Grumman Windstream rotor integrated into a baseline configuration diffuser. It is not an optimum design configuration or size. This diffuser is designed as an aircraft type structure, with rib-supported steel skin, and shear loads transferred by pre-tensioned steel cables. Structural design criteria are given in Table B-1. The basic features of this design are outlined in Figs. A-1 and A-2, and shown in an artist's rendition of an installation (see Fig. A-3).

A breakdown of estimated weight of the DAWT 18 made of AISI 1025 steel (exclusive of the turbine assembly and foundation) is given in Table A-1. Its total weight is almost 44,000 pounds of which the diffuser assembly comprises about 70 percent. Low bid price of three estimating organizations for fabrication of a prototype diffuser was about 75 percent of the total cost of the DAWT (less turbine and foundation). Therefore, for the baseline type DAWT, the cost of the one-off prototype diffuser design is approximately proportional to diffuser component weight; the ratio of diffuser fabrication cost to purchased material cost is close to 3 for the steel construction size examined, exclusive of shipping and final erection costs.

Depending on proximity of the factory to the erection site, and labor intensive operations needed for final assembly, the ratio of final in-place DAWT 18 cost to materials cost is between 5 and 6.

In addition to using higher strength materials, Appendix A indicates the possible design improvements to reduce manufacturing costs, which can bring about a labor cost reduction in this category of up to 50 percent (from a (fabrication/material) cost ratio of 3-4 to a value of 2-3). The additional costs for final assembly, shipping, and erection can be reduced to perhaps the range of a 20 to 40 percent increment on hardware cost. The net result of these considerations for just one redesign approach is a DAWT 18, whose costs are between 40 to 55 percent of the initial point design of mid-February 1978. As shown in Table B-2, this could produce a 60 kW DAWT prototype (rated at 29 mph) with a capital cost of under \$150,000. Depending on the appropriate annual cost fraction, (Refs. 12, B-1) and using the Justus linearized equation (Ref. A-3) for capacity factor, the busbar cost for the prototype DAWT is between 6 and 11 cents per kW-hr.

**TABLE B-1 DAWT STRUCTURAL DESIGN CRITERIA**

Wind Velocity:	120 mph
Gust Factor:	1.21 (U.S. Dept of Commerce)
Wind Direction:	Head-On and Lateral
Allowable Stress:	0.60F <sub>CY</sub> (AISC Spec)
Yield Stress:	36,000 psi (AISI 1025 Carbon Steel)
Ultimate Factor of Safety:	55,000/21,600 = 2.55
Ice/Snow Loads:	Not Included
Turbine Blade Passage Frequency:	12.5 Hz
1109-001W	

**TABLE B-2 DAWT 18 COST PROJECTIONS (1978 \$)**

Description	Category	Prototype Unit	10th Unit	100th Unit	
First Design Study (36,000 psi Y.S. steel Diffuser weight ≈ 44,000 lbs)	Material & parts	\$ 41,000	\$ 41,000*	\$ 41,000*	*No quantitative reduction assumed for quantity involved
	Manufacturing labor cost	113,000	79,000	56,500	
	Assy, Shipping & erection cost	97,000	56,000	49,000	
	Sub total	251,000	176,000	146,500	
	Turbine cost	25,000	24,000	20,000	
	Total cost	\$276,000	200,000	166,500	
One Parametric Redesign possibility (160,000 psi Y.S. steel Diffuser weight ≈ 9000 lbs)	Material & parts	\$ 20,000	20,000*	20,000*	
	Manufacturing labor cost	60,000	42,000	30,000	
	Assy, transp. & erection	30,000	21,000	15,000	
	Sub total	110,000	83,000	65,000	
	Turbine cost	25,000	24,000	20,000	
	Total cost	\$135,000	\$107,000	\$ 85,000	
Busbar Cost of Energy		\$/kW-hr			
(60 kW rated power @ 28 mph, CF = 0.43; V = 18 mph)		0.110	0.088	0.070	18.5% annual cost fraction (private utility)
		0.060	0.047	0.038	10% annual cost fraction (federal agency)
45 kW rated power @ 26 mph, CF = 0.49; V = 18 mph)		0.129	0.102	0.081	18.5% annual cost fraction (private utility)
		0.070	0.055	0.044	10% annual cost fraction (federal agency)
1109-002W					

Estimates of DAWT 18 costs for quantity production of 10 and 100 units, using the 90 percent learning curve slope discussed previously, yield the figures of Table B-2. For the 100th unit, the DAWT 18 busbar cost of energy should be between 4 and 7 cents per kW-hr. It should be further noted that the DAWT size and power rating presented in this example are not fully optimized. Therefore, even better economic results may be expected than those presented in Table B-2's data.

With an augmentation factor,  $\bar{r}$ , of 6, (projected from test results described in the body of this report) the incremental cost of the diffuser will yield the effective power rating of  $(\bar{r}-1) = 5$  additional unducted, low rotor cost (Windstream type) turbines of the same rotor diameter. But the capacity factor of the DAWT could well be 150 percent of that of the Windstream type wind turbine of the same power rating. Therefore, the annual energy output of the DAWT will be the equivalent of  $(1.5 \bar{r} - 1) = 8$  additional Windstream type wind turbines of the same rotor diameter. Similarly, using the same turbine, the busbar cost of energy for the DAWT will be reduced relative to the Windstream turbine by the index

$$I_{BC} = (1/9) \left( 1 + \frac{\text{Diffuser Cost}}{\text{Turbine Cost}} \right) = (1/9) (1 + CR)$$

Lower busbar cost will result when the cost of the diffuser is less than eight times the unducted Windstream type turbine cost. This criterion sets one cost target for the diffuser.

Extending the conditions of DAWT comparative costs to a conventional turbine of equal power rating (but not of the extruded blade, low cost technology rotor design), results in a second type of comparative index

$$I_{BCP} = \frac{c_D + c_{TW}}{c_T} \times \frac{CF}{(CF)_D}$$

where

$c_D$  = Diffuser cost

$c_{TW}$  = Windstream type turbine cost

$c_T$  = Conventional wind turbine cost of equal power rating to DAWT

$C_F$  = Plant factor for conventional wind turbine

$CF_D$  = Plant factor for DAWT

In the more usual situations,  $CF/CF_D$  will be about 0.7 and  $c_{TW}/c_T \ll 1/2$ . Therefore, lower energy cost will result if the diffuser cost,  $c_D$ , is less than the cost  $c_T$  of the conventional but larger diameter turbine system.

For the specific data presented in Table B-2, the less than fully optimized DAWT offers lower busbar energy cost where the average price of conventional 60 kW wind turbines exceeds \$1100/kW in quantities of 100 (and \$1400/kW in quantities of 10). Studies for power ratings less than 100 kW presented



in Ref. B-1 (pages 4-74 and 4-78) assume it reasonable and likely to have capital costs on the order of \$2000/kW for mass produced (10,000 quantity) small wind turbines. Data for actual larger WECS systems are on the order of \$1800/kW installed cost, for the Mod-1 (200 foot rotor diameter) (Ref. B-2) WECS configuration.

We believe this example shows that the DAWT advanced concept is economically viable, and offers a current and practical approach to making wind energy cost-competitive.

#### REFERENCES

- B-1 Coty, U., "Wind Energy Mission Analysis, Final Report," ERDA Report SAN/1075-1/1, Lockheed - California Co., Burbank CA, September 1976.
- B-2 Barchet, R. J., "MOD-1 Wind Turbine Generator Program," Proceedings Third Biennial Conference and Workshop on Wind Energy Conversion Systems, DOE Document CONF-770921, Vol. 1, September 1977, pp. 76-85.

## APPENDIX C

### SURFACE PRESSURE DISTRIBUTION

The engineering design of a prototype field test diffuser has raised questions regarding the proper static pressure load distribution - assumptions which are important to structural design. It has been considered a priori that the severest wind loads on the structure occur when the diffuser is yawed 90 degrees to the prevailing wind. Classic wind tunnel data on cylindrical solid bodies are shown in Fig. C-1, taken from Ref. C-1. The pressure coefficient varies with circumferential angle from the forward stagnation point, and with Reynolds Number.

The sinusoidally varying theoretical curve of Fig. C-1 is the laminar variation described in Appendix A, and is used as the wind loading distribution for stress analysis of the engineering design. The most severe loading condition appears at 90 and 270 degrees to the wind vector, where the local surface pressure is three times the dynamic wind pressure, and is directed radially outward. However, it is evident from the data shown that much lower surface pressures, by up to a factor of three, exist for turbulent Reynolds Number operation at values above  $10^5$ .

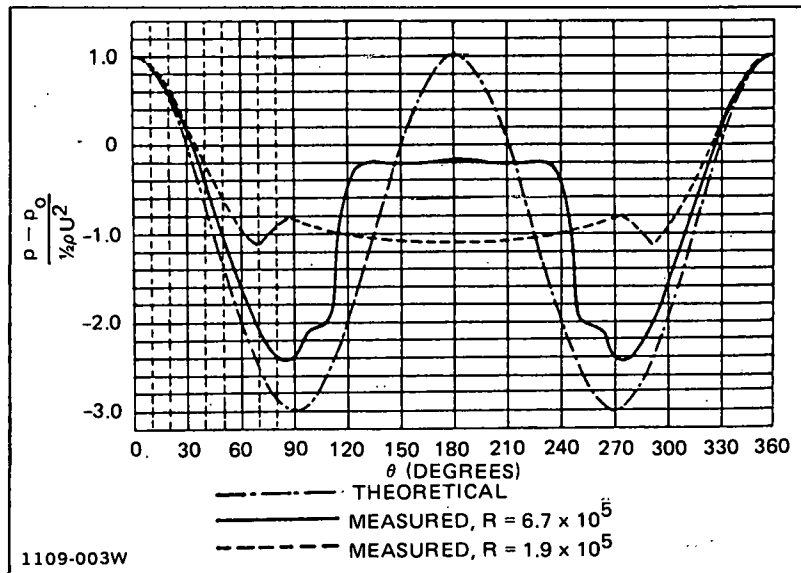


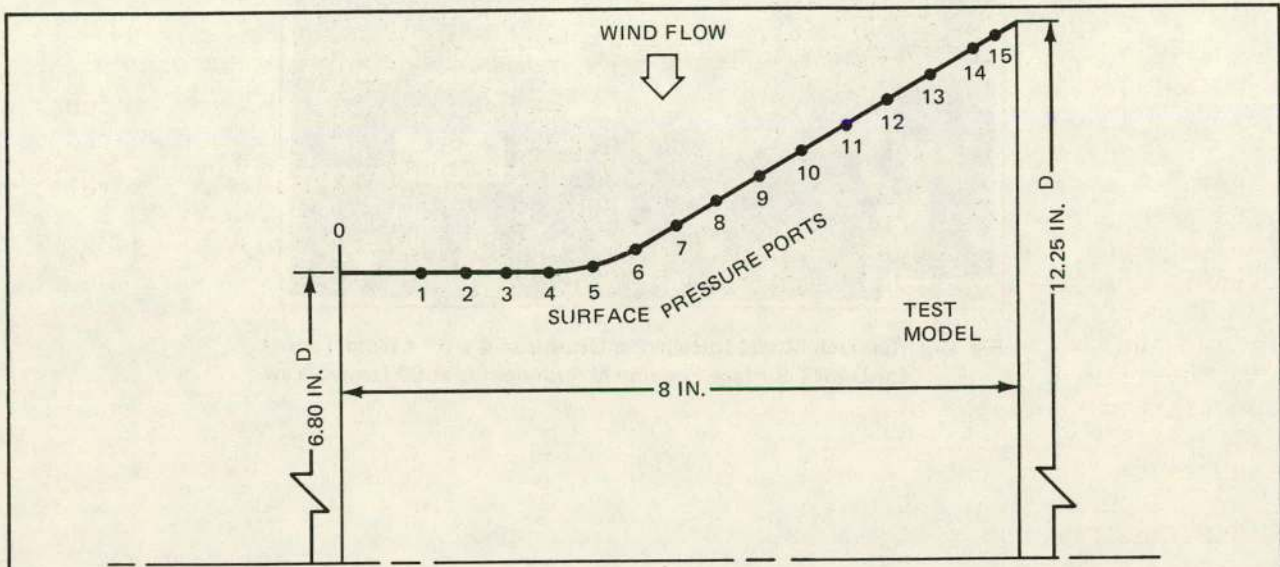
**Fig. C-1 Surface Pressure Distribution on a Solid Cylinder (After Flachsbart, Ref. C-1)**

The specific point investigated by a wind tunnel test series was the applicability of the surface pressure obtained with cylinders, to the truncated conical form of the diffuser used in the DAWT. Testing was conducted in the 4 x 6 ft (1.2 x 1.8m) test section of the research wind tunnel. A 6 in. (15 cm) inlet diameter model, made from an aluminum spinning, was instrumented with fifteen static pressure ports normal to the local outer surface, and running in a line along the full length of the model. The 8 in. (20.3 cm) long model had a 2.5 in. (6.3 cm) long cylindrical section, followed by a curved transition to the 60 degree included angle cone to an exit diameter of 12.25 in. (31.1 cm). As seen in Fig. C-2, the first four static pressure measurements are on the conical section. Pressure ports 5 and 6 are in the transition section, and ports 7 through 15 are located in the conical portion of the model. The pressures were measured sequentially, in sets of five, by means of a scanivalve that connected one port at a time with a single master pressure transducer. Measurements were documented on a chart recorder during a thirty second interval at each port; response time of the system was determined to be five seconds. Angular variation of pressure was obtained by rotating the entire model, in 30 degree increments, about its centerline for a fixed wind speed condition. Figure C-3 shows the model supported by a centerline-located bar perpendicular to the flow direction of the tunnel; the line of static pressure ports are set 30 degrees above the side stagnation location in this picture. At the 26 fps (7.9 m/s) operational airspeed of the facility, the average Reynolds number of the tests (based on model cross-sectional diameter) is about  $10^5$ . The apparent Reynolds number was increased in some tests by a single lengthwise turbulence trip (see Fig. C-4) made of No. 60-1/2 coarse sandpaper strips, 1 in. (2.5 cm) wide by 1 mm thick. These trips were attached at 15, 45, or 75 degrees to the flow direction.

Results of the investigation are given in Figs. C-5 through C-7. The first series of plots of angular distribution of pressure coefficient, Figs. C-5 a,b,c, show that the most severe pressure loading is about one dynamic pressure head radially outward, at about 70 and 290 degrees, from the stagnation position. This loading is one-third of the magnitude indicated by laminar theory. The data further show that the cylindrical portion of the model, ports 1 to 5, has more severe loading than the truncated conical portion, ports 8 to 15, especially as the downstream end of the cone is approached (ports 12 to 15). Presumably, this effect is caused by the lateral component of the cross flow induced along the cone. Figure C-6 shows that placing an end plate between ports 5 and 6 prevents the cross flow of the prior tests, and gives a pressure distribution that is closer to cylinder data given in the literature for the turbulent flow regime condition. The lowest magnitude of pressure shown at port position 5 is probably due to the influence of the end plate.

The results of pressure measurements with trips placed at different angular positions is shown in Figs. C-7 a through i. There is no significant difference in the pressures when the boundary layer trips are placed at 15, 45, or 75 degrees to the mean flow direction. Therefore, we may infer that the untripped boundary layer tests were also for fully turbulent flow conditions.

The overall conclusion of this investigation is that the pressure loading on the DAWT, at 90 degree yaw, is at least one-third that previously used in the structural design of the prototype DAWT (see Appendix A). This conclusion is further substantiated by the determination of overall average drag for the DAWT model, obtained by integrating the measured pressure distribution. The

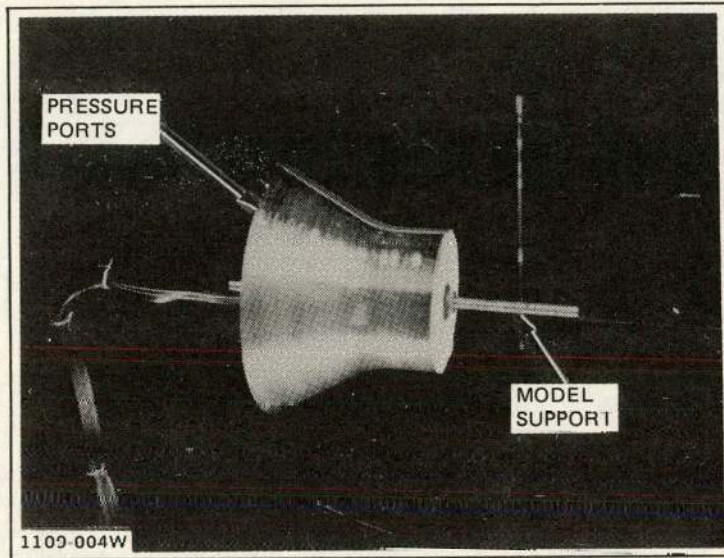


PRESSURE PORT NO.	1	2	3	4	5	6	7	8	9	10	11	12	13	14	15
AXIAL LOCATION, IN.	1.0	1.5	2.0	2.5	3.0	3.5	4.0	4.5	5.0	5.5	6.0	6.5	7.0	7.5	7.75
LOCAL DIAM INITIAL DIAM	1.0	1.0	1.0	1.0	1.02	1.06	1.14	1.21	1.30	1.38	1.47	1.55	1.64	1.73	1.77
RELATIVE AREA RATIO	1.0	1.0	1.0	1.0	1.04	1.12	1.30	1.47	1.69	1.92	2.16	2.41	2.69	2.98	3.14
LOCAL DRAG COEFFICIENT, $C_D^*$	0.61	0.58	0.59	0.61	0.59	0.64	0.60	0.63	0.68	0.76	0.80	0.88	0.94	1.03	1.01
*OVERALL AVERAGE COEFFICIENT = 0.77															

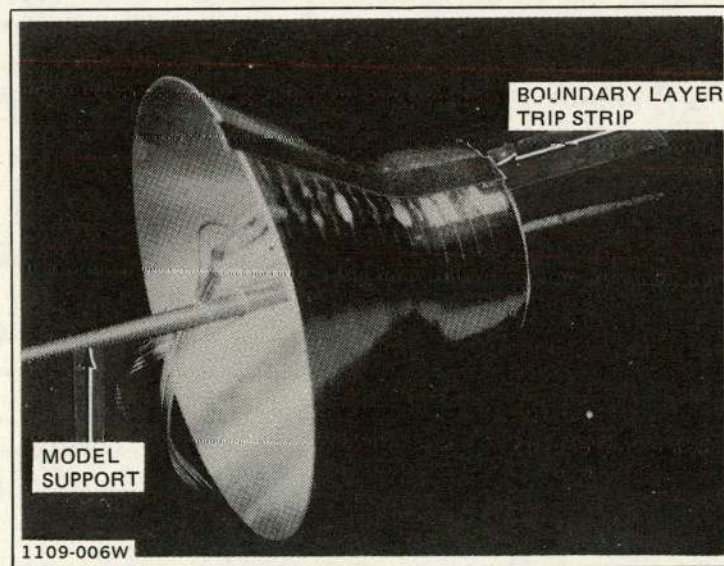
1109-005W

Fig. C-2 Surface Pressure Distribution Model Geometry and Drag Coefficient Data





**Fig. C-3 Research Model Installed in Grumman 4 x 6 Ft Wind Tunnel for DAWT Surface Pressure Measurements at 90 Degree Yaw**



**Fig. C-4 Closeup of DAWT Model for Surface Pressure Distribution Measurements With Boundary Layer Trip Strip Installed**

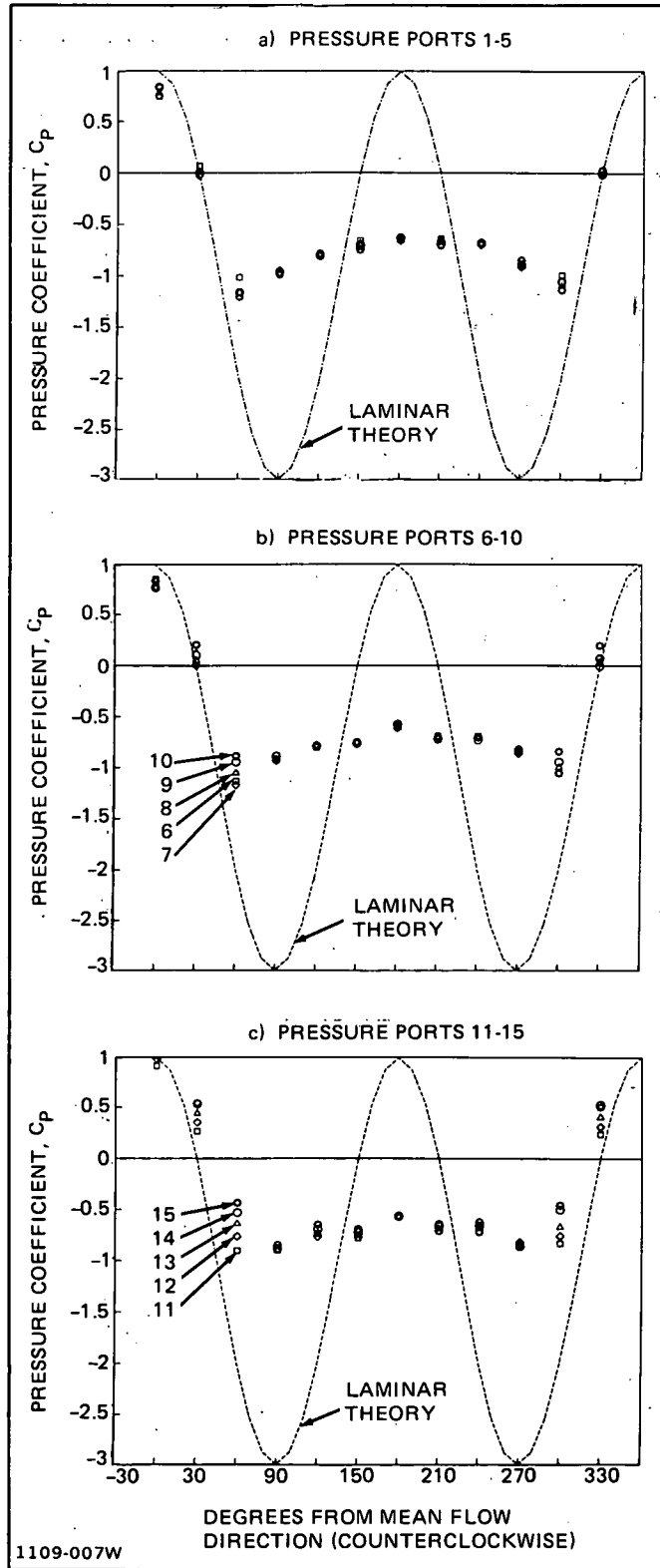


Fig. C-5 Exterior Surface Pressure Distribution on DAWT Model,  $Re \approx 10^5$

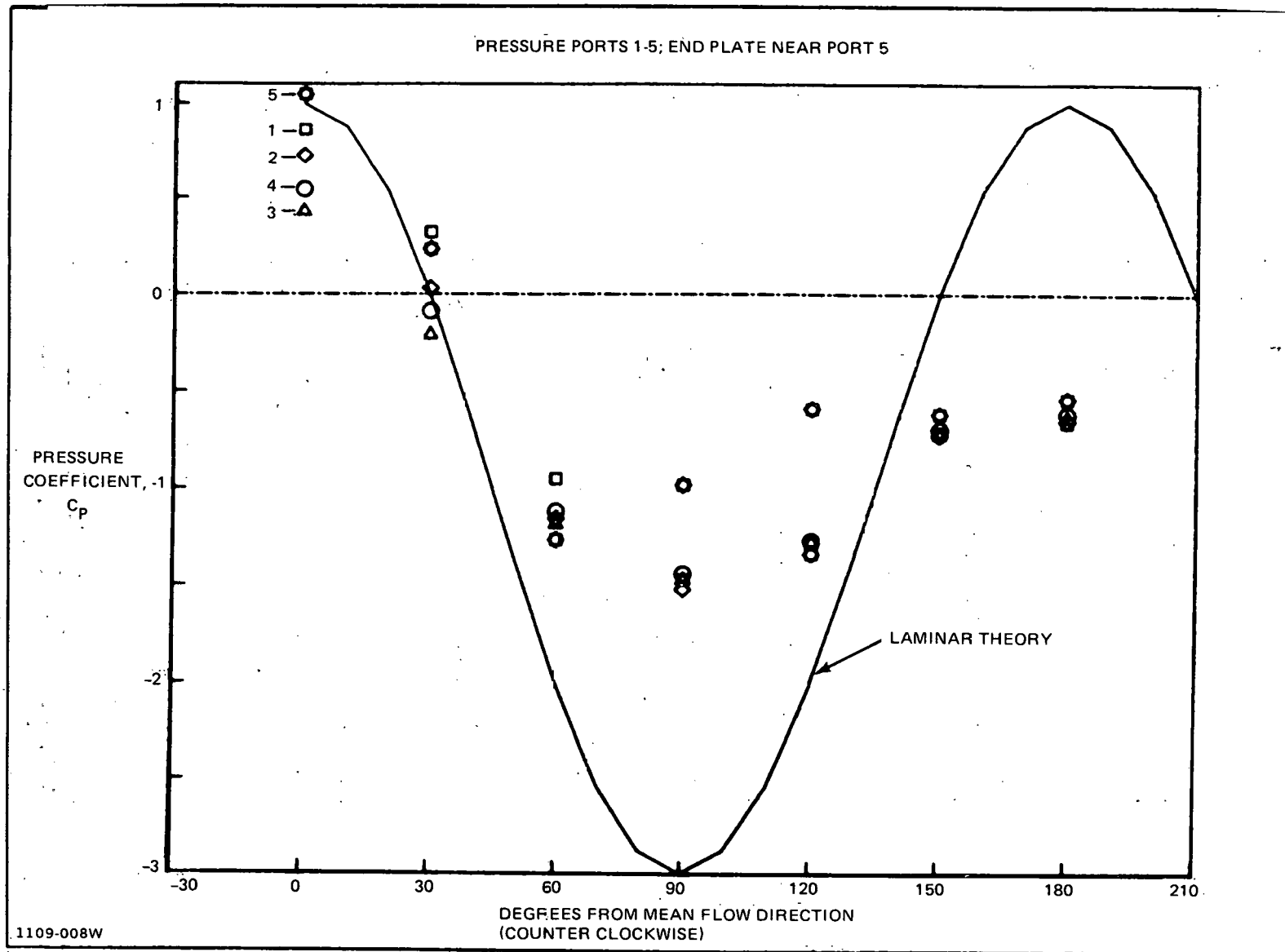


Fig. C-6 Effect of End Plate on Exterior Surface Pressure Distribution on DAWT Model,  $Re \approx 10^5$

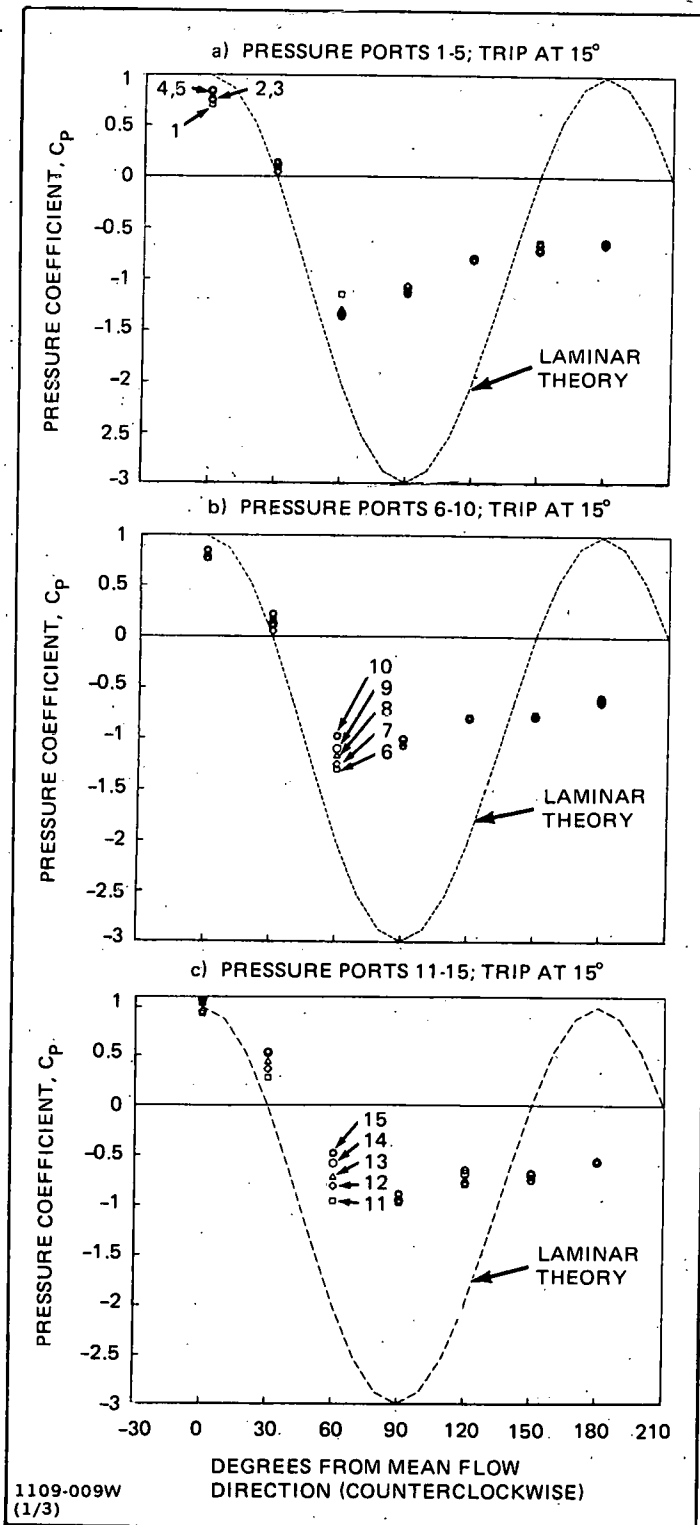


Fig. C-7 Effect of Turbulence Trips on Exterior Surface Pressure Distribution on DAWT Model,  $Re \approx 10^5$  (Sheet 1 of 3)



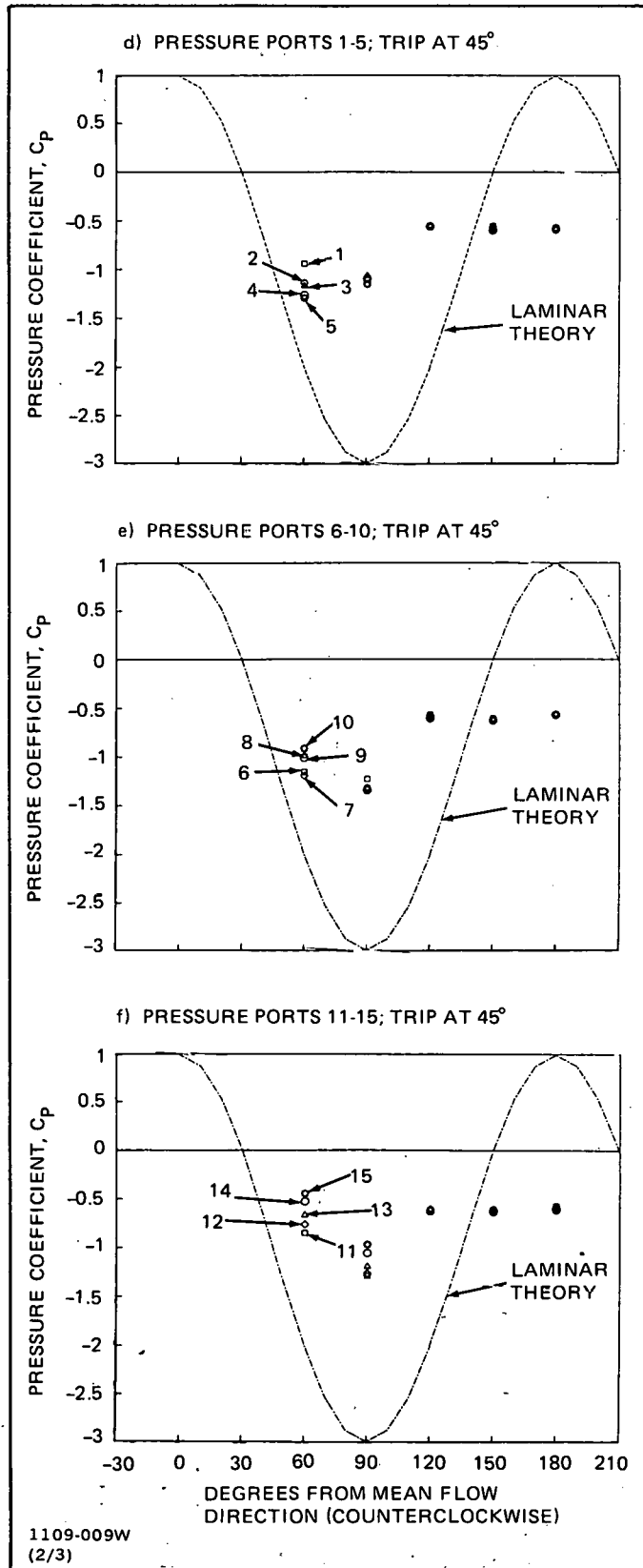


Fig. C-7 Effect of Turbulence Trips on Exterior Surface Pressure Distribution on DAWT Model,  $Re \approx 10^5$  (Sheet 2 of 3)

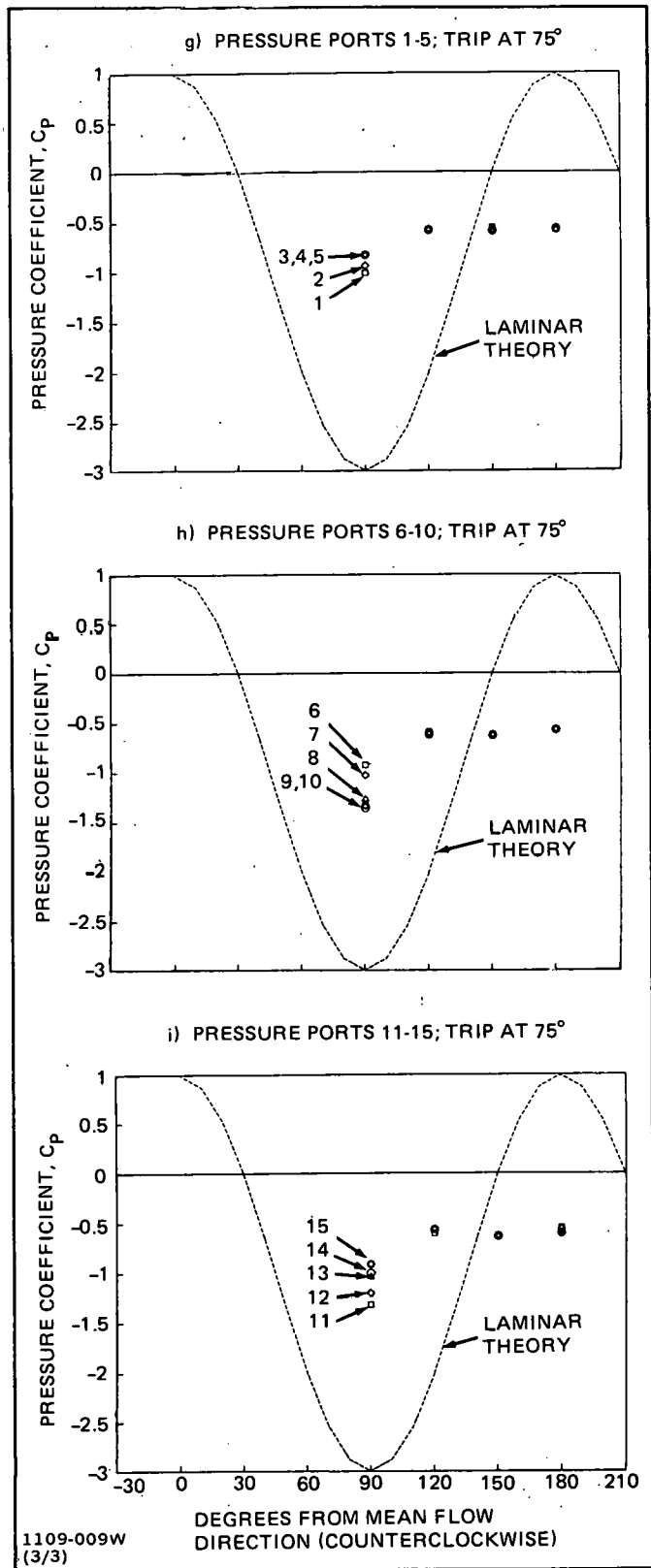


Fig. C-7 Effect of Turbulence Trips on Exterior Surface Pressure Distribution on DAWT Model,  $Re \approx 10^5$  (Sheet 3 of 3)

average drag coefficient determined from these tests is 0.77, which compares favorably with the accepted value of 0.30 for infinite aspect ratio cylinders in fully turbulent flow, and contrasts with the 1.2 drag coefficient for laminar flow over cylinders. These results also compare favorably with the 90 degree yaw condition force measurements (drag coefficient = 1.0) made in the 7 x 10 ft (1.2 x 1.8 m) wind tunnel using a larger (18 in. (46 cm) diameter inlet) DAWT model.

This reduced loading requirement should result in a lighter and cheaper diffuser structure.

#### REFERENCE

- C-1 Goldstein, S., ed, "Modern Developments in Fluid Dynamics," Vol. II, Oxford Press, London, 1938, pps. 421-426.